universität wien

MASTERARBEIT / MASTER'S THESIS

Titel der Masterarbeit / Title of the Master's Thesis

"Cellular Labelling of Individual Neuronal Cells in the Axolotl Brain and Embryonic Tissue"

verfasst von / submitted by

Philipp Marius Weiss

angestrebter akademischer Grad / in partial fulfilment of the requirements for the degree of

Master of Science (MSc)

Wien, 2023 / Vienna, 2023

Studienkennzahl lt. Studienblatt / degree programme code as it appears on the student record sheet:	UA 066 878
Studienrichtung lt. Studienblatt / degree programme as it appears on the student record sheet:	Masterstudium Verhaltens-, Neuro- und Kognitionsbiologie
Betreut von / Supervisor:	Univ.-Prof. Dr. Thomas Hummel

Acknowledgement

First and foremost, I would like to express my heartfelt gratitude to Prof. Dr. Elly Tanaka for kindly hosting me in her group at the Research Institute for Molecular Pathology. Her guidance and support were not only foundational for this work but also for the valuable skills and experiences I gained during my time as part of her amazing team.

I would like to extend my gratitude to Prof. Dr. Thomas Hummel from the University of Vienna for his supervision and engaging discussions during the presentation of my results.

A special note of thanks is dedicated to Dr. Yuka Sugiura and Dr. Claudio Polisseni for their wonderful supervision and unwavering support throughout the entire project. Their mentorship was indispensable in shaping the quality and depth of this research. Acknowledgement is also due to Dr. Leo Otsuki for though-provoking discussions that expanded my academic horizons. To the entire team, I extend my heartfelt thanks for their collaborative spirit, unwavering support, and shared passion. The family-like atmosphere they created made my time with them truly special.

Finally, I want to extend my sincere gratitude to my family and friends for their constant support, encouragement, and presence throughout the entire process. A special thanks is dedicated to Alexandra Straßer, who, despite being on the other side of the world, remained a constant source of support.

Abstract

This study explored different labelling techniques to color-code single neurons within the axolotl (*Ambystoma mexicanum*) brain and embryonic neural plate. Initial investigations focused on single-plasmid microinjection in fertilized eggs to evaluate transposon-mediated integration of a genetic cassette into the genome. This allowed long-term expression of fluorescent, membrane-tagged proteins in embryonic development. Subsequently, whole-brain electroporation was used to assess the compatibility of these genetic constructs for integration into neuronal cells. Further experiments demonstrated that single-cell electroporation (SCE) with dextran dye provided a powerful means to explore the structural morphology of axolotl neurons with remarkable single-cell specificity.

These findings confirm the efficacy of SCE in labelling individual neurons within the axolotl brain and embryo. This offers a novel opportunity to explore the structural dynamics of neurons within brain and neuronal growth during embryonic development. Future investigations combining the longevity of the genetic constructs with the efficiency of SCE hold great promise for not only labelling but manipulating axolotl neural activity to advance neurobiology, particularly in the context of neural tissue regeneration.

Contents

ACKNOWLEDGEMENT **3**

ABSTRACT **5**

1 INTRODUCTION **9**

2 METHODS **13**

2.1 AXOLOTL (*AMBYSTOMA MEXICANUM*) 13

2.2 DYES AND GENETIC CONSTRUCTS 14

2.3 MICROINJECTION IN ONE-CELL STAGE AXOLOTL EGGS 15

2.4 WHOLE-BRAIN ELECTROPORATION 18

2.5 SINGLE-CELL ELECTROPORATION 19

2.6 CUBIC CLEARING FOR BRAINS AND EMBRYOS 22

2.7 WHOLE BRAIN IMMUNOHISTOCHEMISTRY 22

2.8 MICROSCOPY 23

3 RESULTS **24**

3.1 GENETIC CONSTRUCTS ENABLE ROBUST LONG-TERM LABELLING IN AXOLOTL 24

3.2 COMPATIBILITY OF DNA CONSTRUCTS FOR NEURONAL LABELLING 28

3.3 LABELING SINGLE AXOLOTL NEURONS IN THE CONTEXT OF THE BRAIN 29

3.4 PRECISE LABELLING IN THE DEVELOPING AXOLOTL EMBRYO 33

4 DISCUSSION **35**

4.1 INSIGHTS AND CHALLENGES IN GENETIC MANIPULATION 35

4.2 SCE - ENHANCING PRECISION IN AXOLOTL NEUROBIOLOGY 37

4.3 SCE - PRECISE LABELLING IN THE AXOLOTL EMBRYO 38

4.4 PROSPECTS IN COMBINING GENETIC CONSTRUCTS AND SCE IN AXOLOTL 39

5 OUTLOOK **40**

6 CONCLUSION 42

7 REFERENCES 44

8 APPENDIX 49

8.1 DEUTSCHE ZUSAMMENFASSUNG 49

8.2 AXOLOTL TRANSGENESIS - HOW TO INJECT EMBRYOS 50

8.3 HOW TO LABEL SINGLE NEURONS IN THE AXOLOTL BRAIN WITH DEXTRAN DYE 55

8.4 CUBIC PROTOCOL FOR ANTIBODY STAINING 58

1 Introduction

Santiago Ramón y Cajal (1852 - 1934) is widely regarded as an eminent figure in the history of neuroscience and his contributions left an indelible mark on the field (Venkataramani, 2010; De Castro, 2019). During the late 19th and early 20th centuries, Cajal's anatomical observations and profound theoretical insights revolutionized the understanding of the nervous system. Alongside his contemporary Camillo Golgi (1843 - 1926), who developed a silver-staining technique to visualize individual neurons within intricate neuronal networks (Ghosh, 2020), Cajal's work heralded a paradigm shift in neuroanatomy.

These contributions were built upon Cajal's formulation of the 'neuron doctrine' (Llinás, 2003). In contrast to the prevailing notion of the nervous system as a continuous reticulum, Cajal proposed that neurons are distinct entities, functionally separated by synapses (Garcia-Lopez, 2010). Through meticulous observations and detailed drawings, Cajal uncovered the intricate structure and synaptic connections between individual neurons. His insights not only shed light on the complex anatomy but laid the foundation for the modern understanding of the nervous system (Peters, 2007; Yuste, 2015).

In modern neuroscience, methods such as electroporation allow for precise and targeted manipulation of neural cells (Luft and Ketteler, 2015; Deng *et al.*, 2023). This acute transfection provides an alternative to rapidly deliver macromolecules into target cells (Karra and Dahm, 2010). By exposing cells to short and controlled electrical pulses, the permeability of the cell membrane is temporarily increased, allowing foreign substances to enter (Furuya *et al.*, 2003; Escoffre *et al.*, 2009; Kumar, Nagarajan and Uchil, 2019). High efficiency and the ability to target specific areas make this approach particularly favorable, as it can be used to deliver a variety of macromolecules and leave cells intact (Weaver, 1995; Potter and Heller, 2018). Electroporation has been essential in advancing the understanding of neuronal development, signaling and plasticity, contributing to the unravelling of the complex mechanisms underlying brain function (Sariyer, 2013). These advancements open new dimensions for the study of neuronal architecture and function, thereby seamlessly linking Cajal's revolutionary work to the scientific challenges of today.

When using these advanced methods, one must recognize their limitations. Whole-brain electroporation (WBE) enables the delivery of genetic material to a wide area of tissue, thereby facilitating the study of large-scale cellular processes and developmental phenomena (Faulkner *et al.*, 2021). Nevertheless, it faces challenges when it comes to the precise labelling of individual neurons.

Therefore, single-cell electroporation (SCE) emerged to improve the sparsity and precision of labelling. By enabling targeted delivery of molecular makers to individual cells, SCE overcomes the challenges of bulk transfection methods (Haas *et al.*, 2002) - properties that make SCE particularly useful for studying phenomena requiring isolation and manipulation of individual neurons (Keener, Cheung and Futai, 2020). The technique utilizes the principles of electroporation to precisely transfect a single cell within a complex network. Unlike WBE, which can result in a heterogenous transfection pattern across the target tissue, SCE ensures rapid delivery of dyes and fluorescent markers to the selected cells (Bae and Butler, 2006; Wang *et al.*, 2010; Zhang, Zheng and Zhu, 2020). This precision enables real-time visualization of cellular morphology and structural shape (Liu and Haas, 2011a). For long-term studies, SCE offers co-introduction of plasmid DNA with mRNA encoding for a transposable enzyme that facilitates stable integration of transgenes into the cell's genome (Hanahan, 1983; Summers, 1996; Tolmasky and Alonso, 2015). The sustained expression of fluorescent proteins allows the color coding of individual cells and therefore tracking neurons (Hossain, Podgorski and Haas, 2015; Echeverri, Fei and Tanaka, 2022). This is due to the use of transposable elements which increases precision and reliability of transgene integration, resulting in consistent and stable labelling (Kawakami, 2007).

For assessing viability, efficacy, and functional impact of genetic constructs intended for subsequent SCE experiments, microinjection into fertilized eggs provides a valuable framework. The method involves injecting plasmids carrying specific genes or regulatory elements into early-stage axolotl embryos (Peron *et al.*, 2020; Schuez and Sandoval-Guzmán, 2023). These plasmids are expressed either episomally or as integrated constructs and provide a rapid means for screening the functionality of plasmids.

For these approaches, the axolotl (*Ambystoma mexicanum*) serves as an attractive model organism (Voss, Epperlein and Tanaka, 2009; Vieira, Wells and McCusker, 2020). Central to its allure is the axolotl's regenerative capacity, allowing it to regrow body parts such as limbs, tail, heart, and nervous system (Gresens, 2004; Tazaki, Tanaka and Fei, 2017; Gross, 2018; Bölük, Yavuz and Demircan, 2022; Lust *et al.*, 2022). Beyond regeneration, the axolotl offers an array of biological advantages that enhance its suitability as a neuroscience model. Notably, adult female axolotls produce hundreds of eggs in a single clutch (Schuez and Sandoval-Guzmán, 2023). This prolific reproduction allows extensive experimental replication and enables the study of neuronal development at various stages (Adamson, Morrison-Welch and Rogers, 2022). Additionally, the translucency of axolotls skin offers the benefit of real-time observation of neuronal morphology without invasive procedures (Keller, Löfberg and Spieth, 1982), a distinct advantage when employing techniques like SCE for precise labelling and tracking of individual neuronal cells. Moreover, the axolotl's well-characterized developmental stages (Schreckenberg and Jacobson, 1975) and ease of husbandry make it an attractive choice for neuroscientific investigations. Neural development may be tracked from embryonic stage through adulthood (*Fig. 1*), providing insights into both early neuronal patterning and later neural plasticity.

By combining SCE with advanced imaging techniques such as fluorescence microscopy, the morphology of individual tagged neurons within the organism's brain can be monitored in real-time (Combs and Shroff, 2017; Hickey *et al.*, 2021). The dissection of axolotl regenerative and neuronal dynamics not only deepens the understanding of species-specific mechanisms, but also potentially uncovers avenues for harnessing regenerative traits and neuronal repair strategies applicable to a wider range of organisms. Genetic and phylogenetic proximity of the axolotl to other vertebrate species (Nowoshilow *et al.*, 2018) strengthen the translational implications of its neurobiological findings.

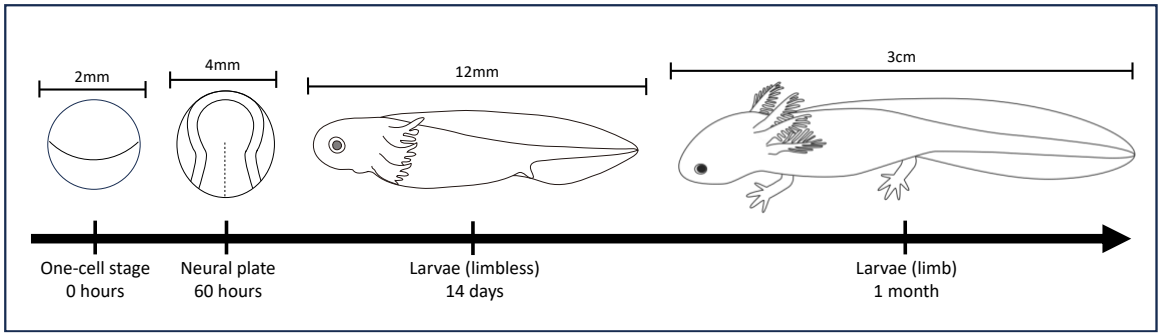

Figure 1: **Developmental progression in axolotl**. This figure illustrates critical developmental stages in axolotls, including freshly laid one-cell stage eggs, stage 15 embryos displaying an open neural plate, limbless larvae at the hatching stage, and 3cm juvenile. The timescale depicted spans from egg laying to one month post fertilization, with size variations ranging from 2mm to 3cm.

The aim of this study is to enhance the accuracy, specificity, and longevity of labelling individual cells within the axolotl brain. This was done by refining SCE through the utilization of dye markers and transposon-mediated integration of fluorescent membrane-tagged proteins. This approach allows to directly visualize the cellular morphology, providing a more comprehensive understanding of neuronal shape and projections within the brain, potentially revealing variations between different brain regions. By extending SCE to the embryonic stage of the axolotl, it becomes feasible for monitoring the growth of neurons during development and to label all neuronal descendants of a given neuronal progenitor. These advancements may contribute to investigations of neural circuitry and structural changes within the nervous system of the axolotl.

2 Methods

This study explores the intricate neurobiological landscape of the axolotl (*Ambystoma mexicanum*), a species known for its remarkable regenerative capacity. The main objective was to provide a method for a more comprehensive examination of the axolotl neuronal structure. This was approached by microinjection and SCE, allowing the accurate introduction of fluorescent markers. These markers enable precise labelling of individual cells and facilitate the study of morphology, growth patterns, and rewiring in neuronal tissue post injury. This approach combines molecular manipulation and advanced imaging to reveal the mysteries surrounding axolotl neuroplasticity.

2.1 Axolotl (*Ambystoma mexicanum*)

For this study, white (*d/d*) and *Tyr*-KO (*Tyrosinase*-Knockout) axolotls of either sex were used. These strains were bred and maintained in the IMP animal facility, guaranteeing controlled and consistent conditions throughout the experiments. All handling and surgical procedures strictly adhered to the guidelines set by the local ethics committee. The experiments were performed in full compliance with the regulations approved by the Magistrate of Vienna (Genetically Modified Organism Office and MA58, City of Vienna, Austria, license GZ51072/2019/16 and license GZ665226/2019/21). To minimize any potential discomfort or stress, the animals were anesthetized in 0.03% benzocaine (Sigma-Aldrich, E1501) before undergoing electroporation or surgical procedures, ensuring their welfare throughout the study.

For microinjection, freshly laid one-cell stage eggs from *d/d* animals were used (*Fig. 2*). Since axolotls are bilaterians, they undergo a highly coordinated and well-known developmental process (Schreckenberg and Jacobson, 1975). Using eggs before the first cleavage event is critical when conducting genetic experiments in the whole body of the axolotl (Schuez and Sandoval-Guzmán, 2023).

In the context of electroporation within the axolotl brain, *Tyrosinase*-Knockout animals ranging 2.5 to 3.5cm from snout to tail were used. This size range was chosen to optimize accessibility to the brain, as the cranial structure is not yet fully ossified. Furthermore, these yellowish axolotls lack melanophores (Fei *et al.*, 2014), enhancing visibility of the brain through the skin.

For single-cell electroporation within the neural plate and adjustments in other embryo tissues, stage 15 embryos were conducted (Schreckenberg and Jacobson, 1975). This developmental stage offers well-defined neural plate structures (Eagleson and Harris, 1990), ideal for precise electroporation procedures aiming to introduce genetic markers or other molecular agents into individual cells. This allowed for controlled manipulations and systematic observations of neural development and thus representing a critical phase for neurobiological investigations.

2.2 Dyes and genetic constructs

In pursuit of refining single-cell electroporation, dextran dyes (Alexa Fluor 488/555, Thermo Fischer D22910/D34679) were employed for short-term labelling within the axolotl brain. This allowed optimizing voltage, pulse duration, and frequency for precise and effective delivery of markers into individual neurons. Moreover, short-term labelling with dextran dye facilitated real-time visualization and structural observations. Immediate uptake and distribution within neurons gained invaluable insights into the effectiveness of SCE. This guided the optimization of the needle tip shape, ensuring minimal damage to surrounding tissue and maximal delivery to the target cell.

To further achieve enduring and genetically stable cell labelling, DNA plasmids (6516bp) under robust control of a CAGGS promotor (1618bp) were encoded to express different fluorescent membrane-tagged proteins (*mVenus*, *mCherry*, *mTurquoise*, *mSapphire*, and *mGFP*; approx. 720bp).

The hallmark laid in the integration of these color-coded sequences into the host genome. This was accomplished by Tol2 sites (228bp) flanking the transgene sequence (*Fig. 2*). The

Tol2 transposase enzyme immediately translated from an additional Tol2 mRNA molecule ensured binding, cutting, and rapidly efficient integration of the genetic sequences into the genome (Kawakami, 2007; Schuez and Sandoval-Guzmán, 2023).

A pivotal step in the validation process involved microinjection to assess the suitability and functional efficacy of the Tol2-mediated system within the axolotl model. Fertilized eggs served as a critical testing ground to evaluate the robustness and reliability of the plasmid-based genetic manipulation approach in a controlled and systemic manner.

2.3 Microinjection in one-cell stage axolotl eggs

For transgenesis in axolotls (*Fig. 2*), a well-established protocol (*Appendix 8.3*) was followed. Freshly laid axolotl eggs were collected from the breeding tank and stored in a controlled environment at 10°C to maintain their viability. The eggs were then gently poured into a metal sieve (Carl Roth, 8098.1) and thoroughly rinsed with tap water to remove any residual dust. Afterwards, the eggs were immersed in sodium hypochlorite solution (0.3ml of 10% NaClO diluted in one liter tap water) for five minutes and thoroughly rinsed again. After proper disinfection due to dual treatment with sodium hypochlorite, the eggs were transferred into 1xMMR/pen-strep solution. Under a stereoscope (Olympus, SZX10), the jelly layer enveloping the eggs was carefully removed with two sharp tweezers. Dejellied eggs were collected in a Petri dish containing 1xMMR/pen-strep solution, where they were kept refrigerated at 10°C until the microinjection.

All required equipment was arranged systematically. This included the preparation of the injection mix (100ng DNA, 500ng Tol2 mRNA, DNase/RNase-free water up to 10µl), needles (made from Harvard Apparatus, No. GC100F-15 w/filament), a silicone mold (Sylgard 184), small Petri dishes, sterile pipettes (2ml), tweezers for needle breaking, and a stage micrometer (Fine Science Tools, 29025-01). The silicone mold was cleaned with deionized water, followed by thorough rinsing. It was then treated with 70% ethanol and rinsed again with deionized water for proper sterilization. Following this, the mold was filled with 10%Ficoll/1xMMR/pen-strep solution. The injection needle was filled with the

injection solution using a microloader (Eppendorf, 5242956003), fixed in a holder (WPI, MPH6S), and attached to a micromanipulator (Narishige, MN-153). A crucial aspect of the preparation involved breaking the very tip of the needle using tweezers to ensure precise and controlled injection. Bubbles at the needle tip were eliminated during this process. The volume of the injection droplet was adjusted to 5nl using a stage micrometer, ensuring accuracy in the injection process.

Healthy-looking eggs (Schuez and Sandoval-Guzmán, 2023) were carefully transferred into the injection mold, facing up the brown animal pole, which is where the cytoplasm and pronucleus are located. An imaginary line running through the middle extending from the animal pole to the vegetal pole of the eggs was targeted. Freshly laid eggs were directly injected below the vegetal pole, whereas for older eggs, the injection point was aimed towards the middle of the animal pole.

Following injection, the eggs were transferred into 10%Ficoll/1xMMR/pen-strep solution for two hours. Afterwards, the embryos were carefully transferred into a large Petri dish filled with 5%Ficoll/0.1xMMR/pen-strep solution and stored at either RT or in a controlled incubator maintained at 16°C. The next day, healthy-looking eggs were transferred to a 24-well plate containing 0.1xMMR/pen-strep solution and stored at RT or in a 16°C incubator. Two weeks after the injection procedure, transgenic efficiency was evaluated via fluorescence microscopy (Zeiss Axio Zoom.V16) to ensure precision and accuracy. Finally, healthy and positively responding embryos were kept in a tap water environment to facilitate their future development.

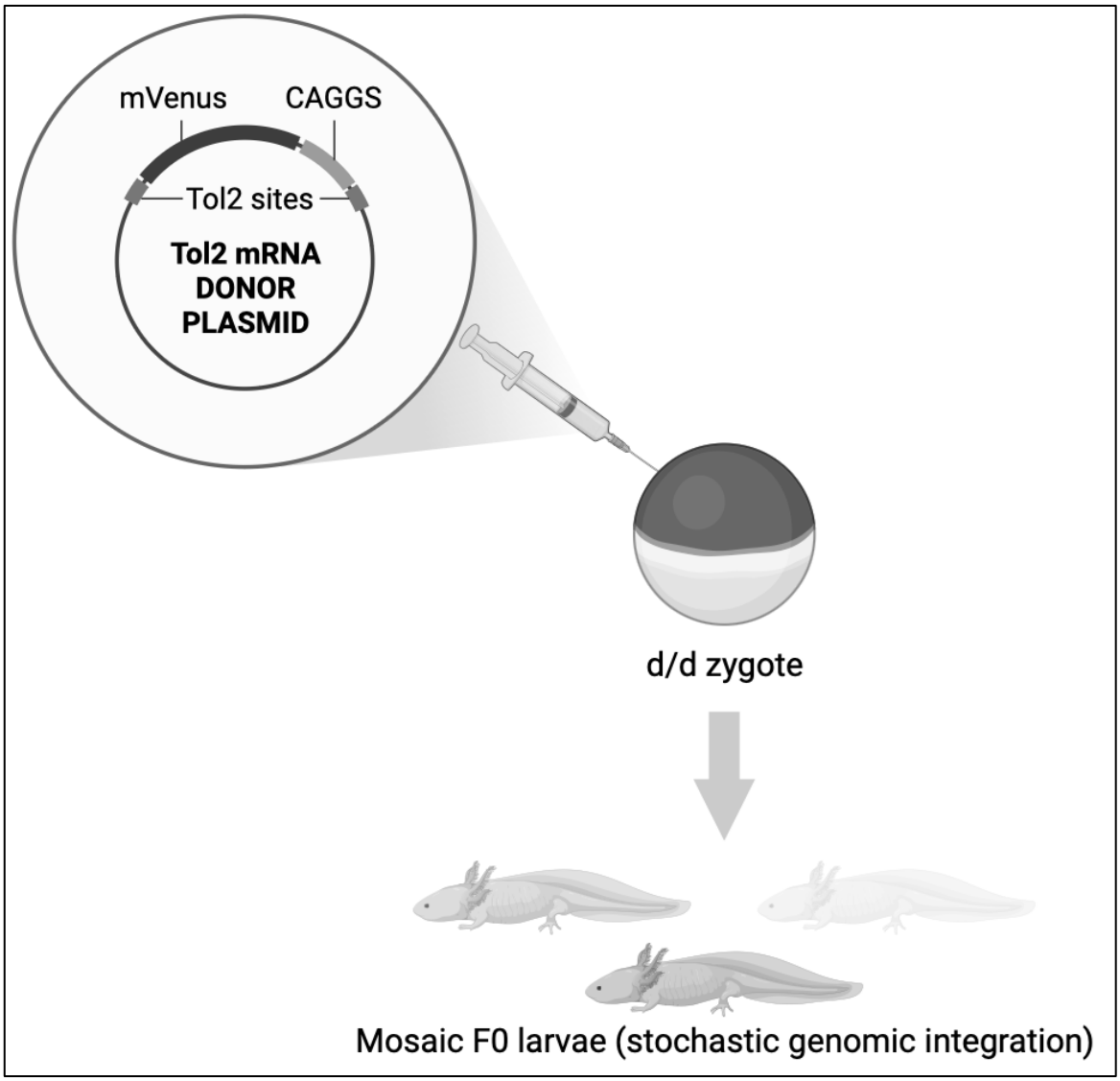

Figure 2: **Transient and stable transgenesis in axolotls.** Transposase mRNA is synthesized via *in vitro* transcription, and plasmid DNA containing Tol2 constructs is co-injected into fertilized one-cell stage eggs. The transposase enzyme produced from the injected mRNA facilitates the excision of the Tol2 constructs from the plasmid and subsequent integration into the axolotl genome. Successful integration, driven by a CAGGS promotor, results in mosaic fluorescence within the injected embryo demonstrating the effectiveness of transient transgenesis in axolotl. (created with Biorender)

2.4 Whole-brain electroporation

Whole-brain electroporation (WBE) was employed as an additional technique to further evaluate the suitability of DNA-transgene integration for neuronal labelling in the axolotl brain. WBE allowed for comprehensive assessment of the constructs' effectiveness in labelling neurons throughout the entire brain (Kunieda and Kubo, 2004; Lust *et al.*, 2022), offering a broader and more detailed perspective on their utility for subsequent single-cell electroporation experiments.

Intraventricular injections of a plasmid encoding for fluorescent membrane-tagged proteins (*mGFP*), diluted in 1xPBS (phosphate buffered saline) at concentrations ranging from 0.5 to 1µg/µl and combined with FastGreen dye (Sigma-Aldrich) to enhance visibility, were performed on anesthetized animals. The procedure took place in a Petri dish under a stereoscope (Olympus, SZX10) for precise visual guidance. The skin covering the brain was carefully removed using a scalpel and tweezers. A glass microneedle (made from Harvard Apparatus, No. GC100F-15 w/filament), controlled by a micromanipulator (Narishige, MN-153), was inserted into the midbrain ventricle and the plasmid solution was injected until the forebrain ventricles were adequately filled. Subsequently, the axolotls were covered with filter paper soaked in 1xPBS, and electroporation was conducted using a NEPA21 electroporator (Nepagene).

For axolotls measuring 3cm from snout to tail (*Fig. 1*), tweezers equipped with round platinum plate electrodes (2mm in diameter) were attached lateral to the head. Unidirectional (+) pulses were applied, beginning with a single 70V pulse lasting 5 milliseconds (msec), which created pores in the cell membrane. This was followed by four 30V pulses, each lasting 50msec, facilitating the precise transfer of injected solution into neuronal cells in a wide area of the brain. A 999msec pause separated each transfer pulse, and the power decreased by 10% with each successive pulse. Following this procedure, the skin was carefully replaced to its original position. The axolotls were then individually housed in cups (A.Hartenstein, UB10), and one week post-electroporation, the whole brain was dissected, cleared, and analyzed by confocal microscopy.

2.5 Single-cell electroporation

Transitioning from WBE, which allowed to investigate the broad integration of the genetic constructs within the brain tissue, single-cell electroporation (SCE) was performed. This molecular delivery technique required a more precise approach (*Appendix 8.4*). The electrical setup as presented in *Figure 3* necessary for performing SCE included a stimulator (A-M Systems Isolated Pulse Stimulator Modell 2100), an oscilloscope (Tektronix TBS 1000C Series Digital Oscilloscope), and a micropipette holder (World Precision Instruments, MPH6R15) equipped with a silver wire electrode designed for insertion into the needle. The stimulator was connected to the silver wire electrode situated inside a glass micropipette containing an internal conducting solution. The other lead from the stimulator was linked to the oscilloscope input, which also received input from the external ground inside a Petri dish filled with 1xPBS serving as electrolyte bath. This external ground was essentially a silver wire (World Precision Instruments, AGW1010) that maintained electrical contact with the experimental animal throughout the electroporation process. The circuit was established when the micropipette contacted the electrolyte bath. To perform SCE effectively, a fluorescent stereoscope (Olympus, SZX16) with a sufficient working distance was essential. A generous working distance allowed for maneuverability and permitted the micropipette to be positioned at an angle of approximately 30-45 degree, facilitating precise targeting during the procedure.

The preparation of micropipettes was a crucial step, achieving a narrow tip and ensuring tip durability during tissue punctuation. Borosilicate glass capillaries (Standard wall w/filament G150-2) with an outer diameter of 1.50mm and an inner diameter of 0.86mm served as the foundation for micropipette construction, offering the necessary structural integrity while enabling fluid flow. An internal filament within the glass aided in drawing back-filled fluid toward the tip. The micropipettes were crafted on a horizontal micropipette puller (Sutter instrument P-97) using adjusted settings to get the optimal tip shape (Heat = Ramp, Pull = 0, Velocity = 45, Delay = 1, Loops = 4) for SCE within the axolotl brain. The fabrication process acknowledged that adjustments may be needed to tailor the micropipette tip's shape and diameter to specific tissue requirements outside the axolotl brain.

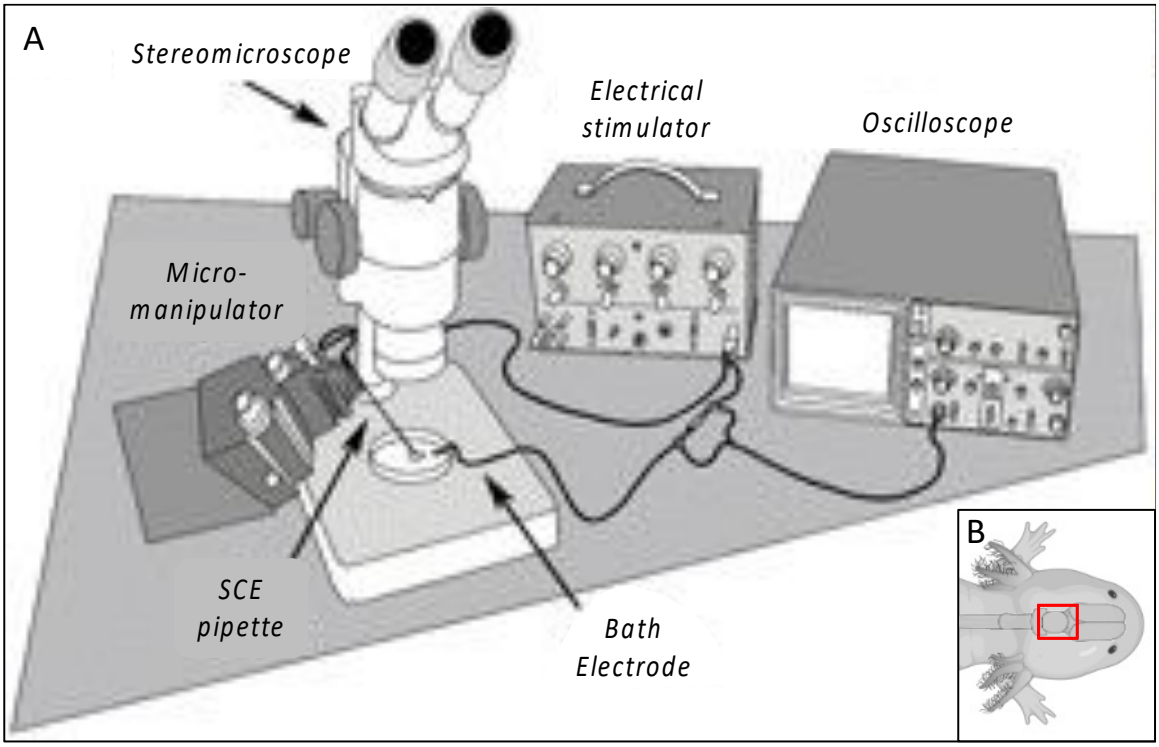

Figure 3: **Setup for single-cell electroporation (SCE)**. (**A**) The electrical setup required for performing SCE consists of a stimulator, an oscilloscope, and a micropipette holder equipped with a silver wire electrode for insertion into the micropipette. The stimulator connects to the silver wire electrode within this micropipette filled with a conducting solution. The other lead links to the oscilloscope input, which also receives input from an external ground placed in an electrolyte bath. This second silver wire maintains contact with the experimental animal throughout the SCE process. The circuit is completed when the micropipette contacts the electrolyte bath. Effective SCE requires a fluorescent stereoscope with a sufficient working distance, enabling precise targeting at an angle of 30-45 degree. (adapted from Liu and Haas, 2011) (**B**) A three centimeter axolotl displaying the CNS, comprising brain and spinal cord, with the optic tectum highlighted by a red square. The optic tectum serves as the target region for SCE due to high density of neuronal cell bodies near the brain's surface.

To adjust the parameters for pulling micropipettes usable for targeted labelling of neuronal cells in the axolotl brain, dextran dye was utilized due to its advantages over genetically encoded fluorescent proteins. Fluorescent dyes offer immediate visibility under epifluorescence, allowing direct observation of the micropipette tip's location within the tissue. This real-time feedback confirmed the correct setup of equipment and the suitability of the micropipette tip for electroporating individual cells. In this context,

micropipettes were filled with the desired compound solution using a microloader (Eppendorf, 5242956003). For fluorescent dextran dyes, the concentration was approximately 300µM and volumes of 2-3µl were sufficient for loading the micropipette. Plasmid DNA was ensured to be endotoxin-free and prepared in water concentrated at 1-2µg/ml. To ensure the cleanliness of the micropipette, solutions containing the desired molecules were briefly centrifuged (LLG-uniCFUGE 2) at high speed to reduce debris that could potentially clog the micropipette. After filling the needle, air bubbles within the tip were removed by vigorously flicking the micropipette, as they could interfere with current flow during electroporation. This guaranteed a smooth and consistent electroporation process. The filled needle was inserted into a micropipette holder mounted on a 3-axis micromanipulator (Narishige, MN-153) and the silver wire electrode was checked to be in contact with the internal solution.

For the SCE procedure, experimental animals (3cm in *Fig. 1*) were anesthetized in 0.03% benzocaine. A single axolotl was gently transferred into the electrolyte bath under the stereoscope. The head of the axolotl was carefully exposed by making an incision behind the optic tectum (red square in *Fig. 3*) with a scalpel, and sharp tweezers were used to open the skull providing access to the optic tectum region. This area was chosen based on its high density of neuronal cell bodies (Maden, Manwell and Ormerod, 2013). Under microscopic guidance, the micropipette was positioned above the targeted region and slowly lowered until it touched the brain's surface. For SCE using fluorescent dextran dye, one negative square pulse with a duration of 30msec and a voltage of 15V was employed to efficiently label neuronal cells within the optic tectum. After stimulation, the pipette was withdrawn, repositioned to another site in the brain area, and the process was repeated. Multiple sites were electroporated in each hemisphere while ensuring that labelled cells did not overlap. The axolotl was returned into a container with tap water to recover, and the procedure was repeated with another anesthetized axolotl. Subsequently, for screening purposes, axolotls were anesthetized once more in diluted benzocaine and placed in a Petri dish. The animals were rapidly screened for successful labelled cells with an epifluorescence microscope (Zeiss Axio Zoom.V16).

2.6 CUBIC clearing for brains and embryos

To obtain detailed high-resolution images of DNA-injected and electroporated brains, the presence of substantial yolk in the head rendered direct tissue imaging ineffective. This necessitated the exploration of a suitable clearing method to distinctly visualize the expressed signal (*Appendix 8.4*; Matsumoto *et al.*, 2019). Therefore, the brain of injected animals was dissected and fixed (4% paraformaldehyde, PFA) over night at 4°C.

Following overnight fixation in 4% PFA, six 30-minute washes with PBST (0.2% Triton) were conducted, effectively eliminating any residual fixative. To mitigate potential autofluorescence originated from blood cells, depigmentation was carried out by immersing the specimens in a freshly prepared bleaching solution (6ml H_2O_2, 1g KOH, PBST up to 200ml) for approximately one hour on a shaker at room temperature (RT) with an intermediate evaluation after 30 minutes. Subsequently, the samples underwent three 10-minute washes in PBST at RT.

Delipidation was achieved through a two-step process, commencing with immersion in a 50% CUBIC-L/R1a solution (see *Appendix 8.4*), initially prepared in a 1:1 ratio and further diluted to 50% with distilled water (dH_2O). After 30 minutes on a shaker at RT, the samples were transferred into 100% CUBIC-L/R1a solution and incubated for one hour on a shaker at 37°C. Next, the specimens were washed four times 20 minutes with PBST at RT, thereby refining tissue quality even further. The ultimate step revolved around achieving refractive index (RI) matching. This was accomplished by immersing the samples in CUBIC-R+(N) solution and allowing them to remain on a shaker at RT until reaching a state of transparency, signaling their readiness for subsequent analysis.

2.7 Whole brain immunohistochemistry

To substantiate the successful tissue labelling, antibody staining was carried out during the CUBIC clearing protocol (*Appendix 8.5*) after delipidation. Following this step, samples were washed four times with PBST at RT for 20 minutes each. Subsequently, blocking was performed by incubating the specimens in a solution containing 4% goat serum (Thermo

Fisher Scientific, 16210072) and 1% DMSO (dimethyl sulfoxide) in PBST for one hour on a shaker at RT. Next, the antibody was applied in a solution of 4% goat serum and 1% DMSO in PBST, followed by six nights at 4°C. After incubation, samples underwent six 30-minute PBST washes on a shaker at RT. Finally, samples were immersed in RI matching solution and kept on a shaker at RT until achieving transparency. This study used HuC/D (Thermo Fisher Scientific, A-21271), a pan-neuronal antibody, to stain neuronal cell bodies within brain tissue.

2.8 Microscopy

Cleared and stained brains were carefully mounted in glass-bottom dishes (Ibidi, 81158) and imaged using an inverted Zeiss LSM980 Axio Observer confocal microscope equipped with a 10x/0.3 plan-apochromat DIC objective. For screening purposes, a Zeiss Axio Zoom.V16 microscope was employed, while single labelled neurons (SCE) were imaged by a custom-built upright 2-photon microscope to achieve higher resolution. The ZenBlue 3.2 software was utilized for image acquisition, and FIJI (based on ImageJ 1.53t) for subsequent image processing and preparation.

3 Results

Building upon the optimized methods described in the preceding section, this study embarked into the intricate neurobiology of the axolotl (*Ambystoma mexicanum*). The goal was to develop a method enabling comprehensive exploration of the axolotl's neuronal structure. This involved microinjection and single-cell electroporation for precise introduction of genetic markers and dyes. These macromolecules allowed targeted labelling of individual cells, providing a powerful tool to investigate morphological changes, growth patterns, and neuronal tissue rewiring post injury. This approach seamlessly combined molecular manipulation with state-of-the-art imaging techniques, unveiling neuronal morphologies within the axolotl nervous system.

3.1 Genetic constructs enable robust long-term labelling in axolotl

To assess usability and long-term expression of plasmids carrying various fluorescent membrane-tagged proteins (*mVenus*, *mCherry*, *mTurquoise*, *mSapphire*, and *mGFP*), driven by a strong, ubiquitous CAGGS promotor, along with Tol2 mRNA, microinjections were performed in one-cell stage axolotl eggs. Transposase-mediated integration into the host genome allowed evaluation of mosaic expression during development (*Fig. 2*) to assess the suitability of genetic constructs for long-term electroporation experiments.

Transposase enzymes, synthesized from Tol2 mRNA, orchestrated the cleavage of the transgene (*Fig. 2*) and its integration into the host genome. The variable expression of fluorescent proteins among cells stemmed from this stochasticity and integration into the genome at various developmental stages after the one cell stage. This resulted in diverse mosaic signal patterns among injected embryos. The expression of these fluorescent proteins was detected in various tissues, encompassing gills, musculature, skin, and cerebral tissue, as shown in *Figure 4*.

Examination two weeks post injection revealed a fluctuating survival rate, ranging from 45% (*mTurquoise*) to 96% (*mVenus*). Notably, this appeared to be predominantly rooted

in egg quality rather than the microinjection procedure, as approximately 89% of the surviving axolotls displayed fluorescent signal (*Table 1*). The fraction of 'positive' animals ranged from 76% (*mTurquoise*) to 100% (*mSapphire*), thereby serving as a clear indicator of transgenesis efficiency. Equally notable, 40% of the survivors and 42% of the 'positive' animals manifested fluorescent signal within brain tissue, underscoring the potential for these constructs in neuronal labelling and confirming widespread expression within the central nervous system (CNS).

To confirm the successful labelling of neuronal tissue, immunohistochemical staining was conducted with an antibody against HuC/D, a panneuronal gene. As an example, a detailed examination of neuronal cell bodies within the right hindbrain region of an embryo that had been injected with mSapphire-carrying plasmids is portrayed in *Figure 5*. Positively identified cells (*in green*) concurrently exhibited co-staining with HuC/D antibody (*in gray*), thereby confirming their neuronal identity. Similar co-labelling results were observed for the other fluorescent proteins. This observation underscores the effectiveness of the genetic constructs in achieving labelling of neuronal tissue, a critical step to harness these constructs for single-cell electroporation experiments.

Furthermore, a cohort of sixteen mVenus-positive individuals was kept over an extensive eight-month period, all of which maintained persistent fluorescent signal, as exemplified in *Figure 6*. This sustained expression of the fluorescent marker serves as evidence for the stability and longevity of the genetic constructs likely caused by Tol2-mediated transposition, rendering Tol2-mediated integration well-suited for extensive studies requiring prolonged genetic labelling and tracking.

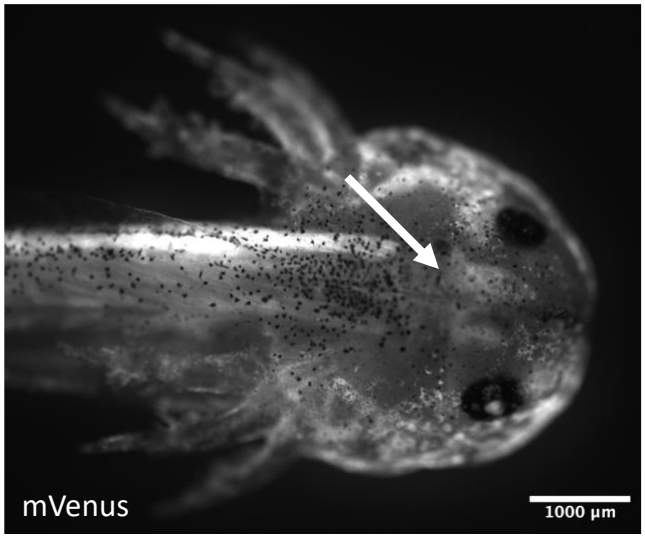

Figure 4: **Axolotl larvae following microinjection of mVenus**. This illustration shows an axolotl that underwent microinjection with mVenus-carrying plasmids. Over a course of two weeks of development, these genetic constructs triggered the expression of mVenus, a fluorescent membrane-tagged protein. Examination using a fluorescent microscope revealed a mosaic pattern of mVenus signal distributed throughout the entire axolotl. Notably, this specimen also displays positive mVenus expression within the brain, as indicated by the arrow. This observation underscores the potential utility of these constructs for neuronal labelling.

Plasmids	Injections	Survivor	Positive (% of survivor)	Brainpositive (% of survivor)
mVenus	154	148	132 (89)	55 (37)
mCherry	90	73	69 (94)	28 (38)
mTurquoise	66	30	23 (76)	13 (43)
mSapphire	54	25	25 (100)	17 (68)
mGFP	62	43	38 (88)	7 (16)

Table 1: **Summary of microinjection experiments in axolotl embryos**. This table provides a concise summary of microinjections carried out using plasmids encoding various fluorescent membrane-tagged proteins along with Tol2 mRNA in one-cell stage axolotl embryos. The table includes details on the total number of injections conducted for each plasmid, the survival rate of embryos assessed two weeks post-injection, the number of animals displaying positive expression of the introduced fluorescent markers, and the corresponding percentage of positive expression in relation to the total survivors. Additionally, the table records the count of embryos with positive expression specifically within the brain and the percentage of brain-positive expression relative to the total survivors. This data sheds light on the applicability of the genetic constructs for electroporation experiments and underscores their functionality and efficacy in axolotl embryos.

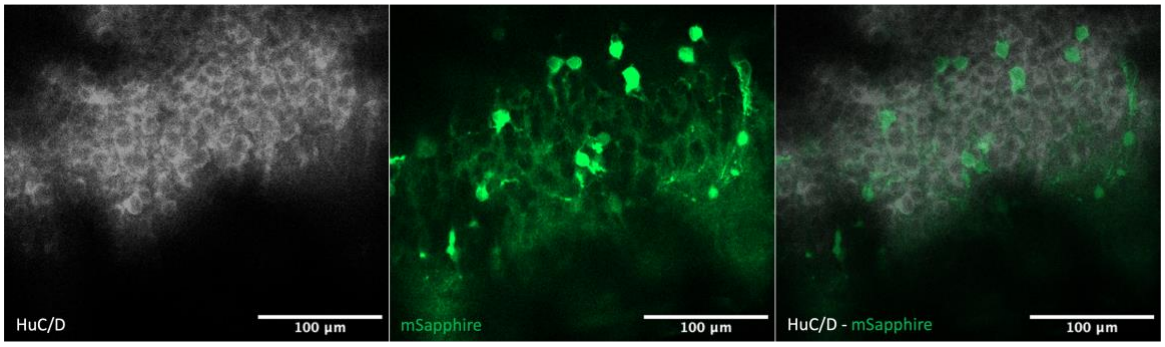

Figure 5: **Evidence of neuronal tissue labelling with genetic constructs**. This figure reveals the results of neuronal tissue staining in axolotls with anti-HuC/D, a panneuronal antibody, following injection of mSapphire-carrying plasmids. The study aimed to verify the successful labelling of neuronal cells within the brain of the axolotl embryo. To achieve this, brains were carefully dissected, and CUBIC cleared to enhance tissue transparency for confocal microscopy. The left image depicts HuC/D-stained neuronal cell bodies within the right hindbrain, demonstrating the antibody's specificity to neuronal cells. In the middle section, the expression of mSapphire within the same neuronal tissue is shown, confirming successful labelling with genetic constructs. The right image displays the overlap of antibody staining and mSapphire expression, providing compelling evidence of co-expression within neuronal cell bodies. These results underscore the effectiveness of the genetic constructs in achieving targeted labelling of axolotl neuronal tissue, a crucial step for their application in single-cell electroporation experiments.

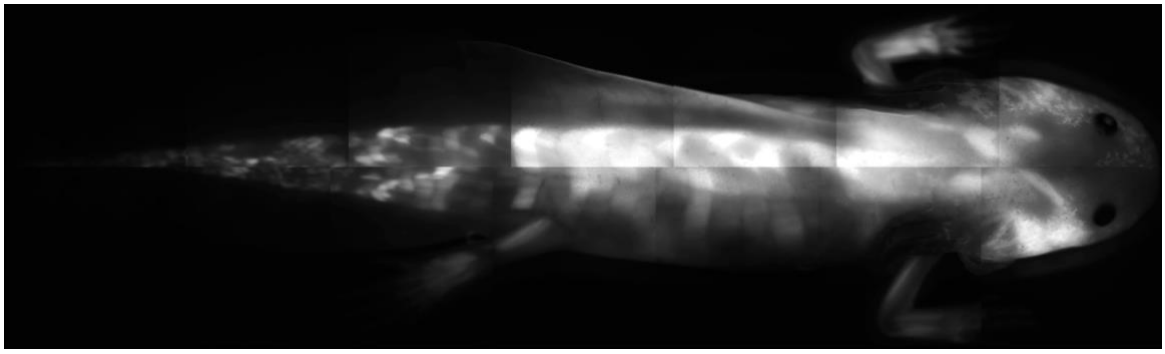

Figure 6: **Long-lasting expression of mVenus in adult axolotl**. This image depicts an 8-month-old axolotl, measuring 14cm in snout to tail, that underwent mVenus Tol2-mediated microinjection. The continuous mVenus signal in this mature axolotl highlights the durability and persistence of the genetic constructs within the axolotl. This long-lasting expression of the fluorescent marker holds particular significance for future experiments, especially those demanding extended genetic labelling and tracking over prolonged periods. These findings provide compelling evidence for the robustness and reliability of the Tol2-mediated approach, further validating its suitability in electroporation experiments and long-term studies.

3.2 Compatibility of DNA constructs for neuronal labelling

Whole-brain electroporation (WBE) was employed to further assess the compatibility of the fluorophore expression with direct cell electroporation into axolotl larvae brain. A plasmid containing CAGGS::mGFP was introduced into the brain's left hemisphere via intraventricular injection and application of unilateral pulses. This effectively transfected neuronal cell bodies and extensively labelled cellular processes (indicated by arrows in *Fig. 7*), affirming the genetic constructs' effectiveness for neuronal labelling. However, as depicted in *Figure 7* (gray arrows), this approach labelled a broad region of the neuronal tissue, limiting the analysis of individual neurons separately.

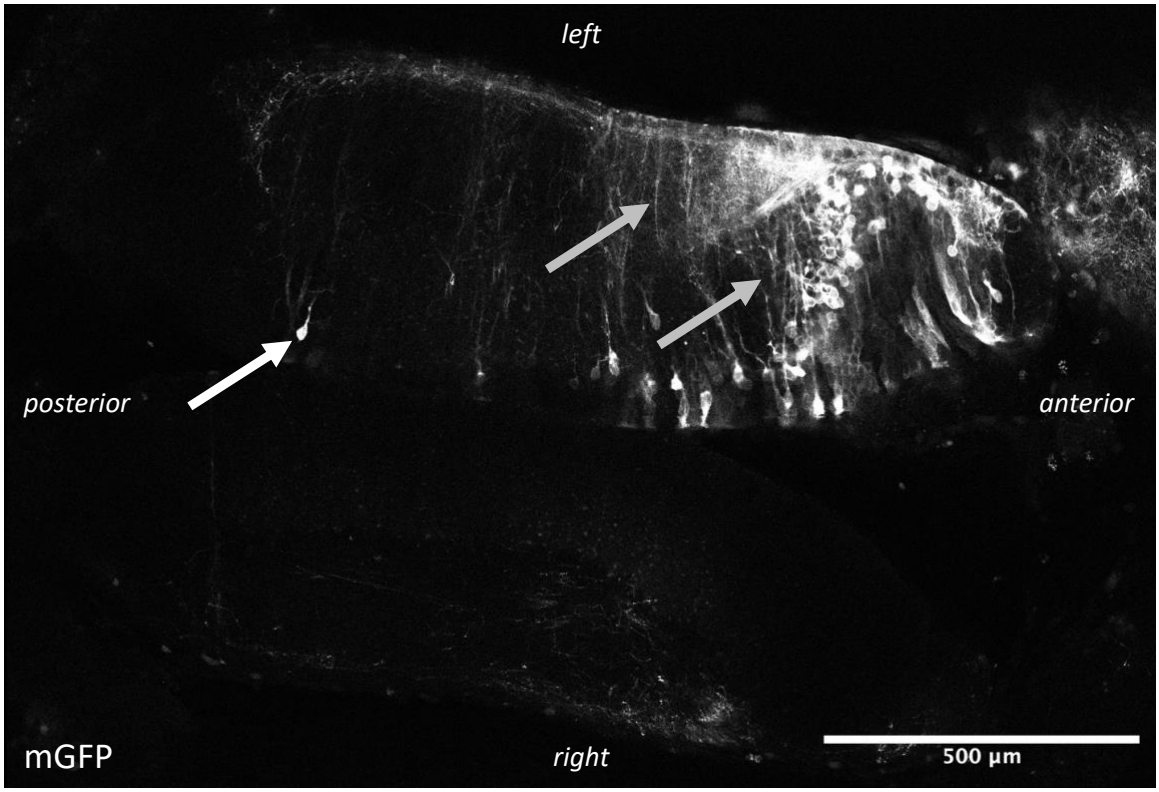

Figure 7: **Whole-brain electroporation (WBE) of mGFP in an axolotl brain**. This image presents an axolotl brain after WBE using mGFP plasmids. The procedure included injecting the plasmid solution into the brain's ventricle and applying unidirectional pulses to enable the integration of genetic material into neuronal cells. The image displays the expression signal of mGFP within the left hemisphere of the axolotl brain.

3.3 Labeling single axolotl neurons in the context of the brain

Unlike WBE, which results in a heterogeneous expression pattern in many cells across the target tissue (*Fig. 7*), SCE ensures precise delivery of material into selected single neurons. This precision facilitates the study of specific neuronal morphology, functions, and connections, a crucial aspect of understanding complex neural networks. SCE also enables the correlation of genetic expression with specific electrophysiological responses, shedding light on the functional role of individual neurons within the broader neuronal landscape. It proves particularly valuable for investigating phenomena that demand the isolation and manipulation of individual cells, providing insights into their responses and contributions to network dynamics.

Initial experiments adopted SCE settings based on those used for *Xenopus laevis* (Hewapathirane and Haas, 2008) as starting point. After opening the skull to access the brain's surface, single neurons within the optic tectum were targeted with dextran dye. As illustrated in *Figure 8*, multiple cells were selected in each hemisphere of the brain, with each labelled cell representing an individual electroporation event. Initial assessments immediately after SCE with dextran dye revealed labelled cell bodies within the optic tectum and processes extending laterally. One hour post SCE, the first signs of axon punctuation emerged, suggesting neuronal cell death. Over a period of three hours, the punctuations extended to the soma and the fluorescent signal ultimately perished shortly after SCE.

To address this challenge, various parameter adjustments were systematically explored (*Table 2*). After extensive experimentation, settings were identified that enabled effective labelling of targeted neurons in the optic tectum for a minimum of four hours (*Fig. 9*). This optimization process involved simplifying parameters to a single pulse of 15V for 30msec. These optimized settings were further validated through live imaging using a 2-photon microscope, as shown in a 16-hour time-course (*Fig. 10*). The results demonstrated enhanced viability of labelled neurons when employing the optimized electrical settings compared to the previous ones. Although the signal eventually fades as the cells died, the decline occurred approximately 12 hours later, allowing for morphological studies and in-

depth evaluations of structural-functional relationships. High-resolution microscopy provides the capacity to zoom in on individual parts of the neurons, facilitating the assessment of potential structural changes due to interactions with other neurons.

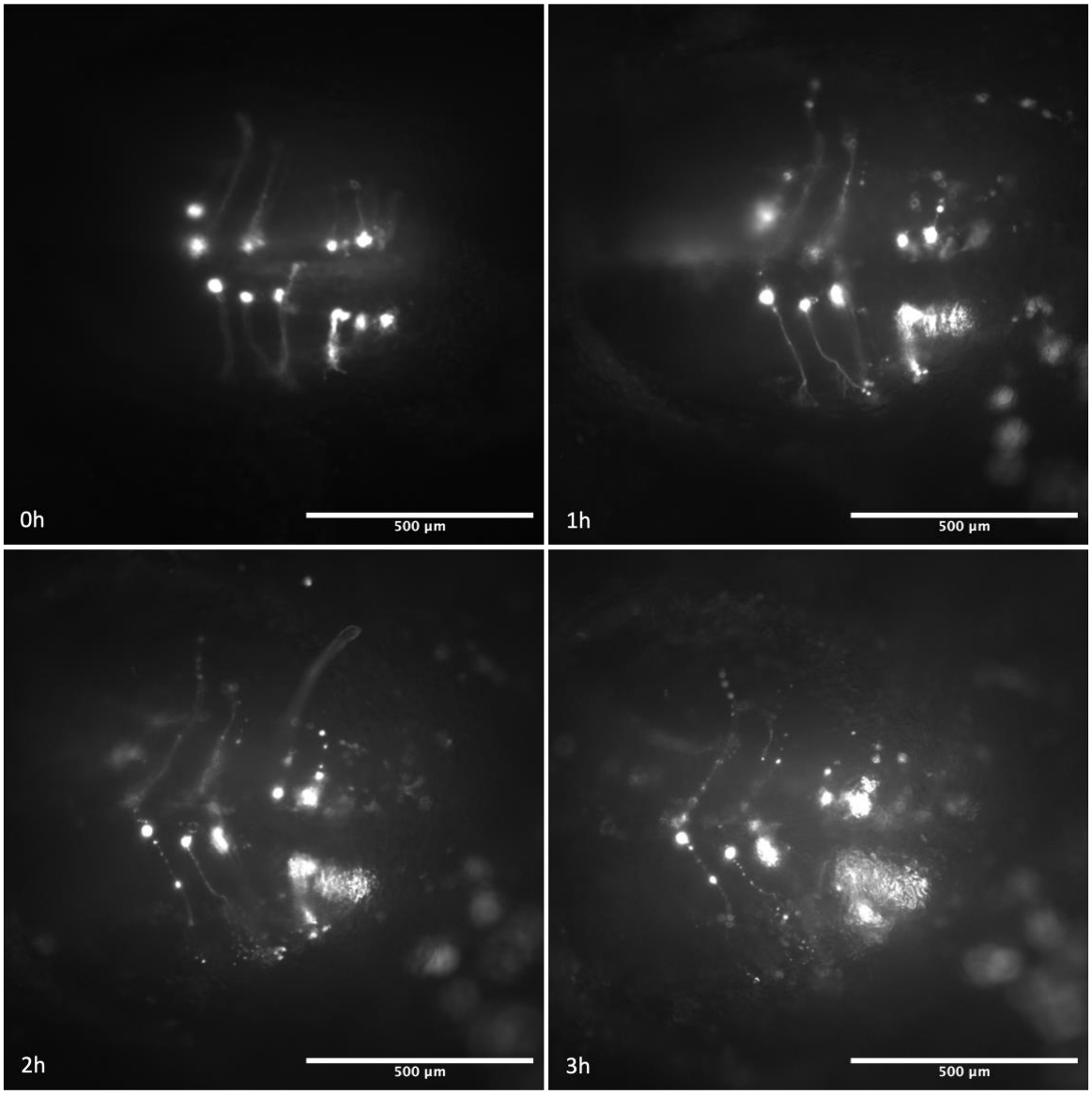

Figure 8: **Time-lapse imaging of dye-labelled neurons in the axolotl optic tectum**. These images capture the dynamic changes in axolotl optic tectum neurons during a three-hour period following dye-labelled single-cell electroporation. Initially, settings adapted from *Xenopus laevis* were employed, resulting in robust labelling with dextran dye. However, as time progressed, the dye signal gradually diminished, and the axons of the labelled neurons exhibited punctuate patterns. This punctuation process continued towards the soma, indicating the degeneration of dye-labelled cells.

Burst duration	***Adjusted to interpulse period and pulse number***							
Pulse duration	**200 µsec**	**1 msec**		**10 msec**	**20 msec**		**30 msec**	**40 msec**
Interpulse period	**1 msec**							
Voltage	**10 V**	**15 V**		**20 V**	**30 V**		**40 V**	**50 V**
Pulse number	**1x**	**2x**	**3x**	**4x**	**5x**	**7x**	**8x**	**10x**

Table 2: **Optimization of single-cell electroporation (SCE) parameters for labelling individual neurons within the axolotl brain**. This table presents the exploration of various SCE parameters to achieve optimal labelling of individual neurons within the axolotl brain using dextran dye. SCE settings were adapted from previous work done in Xenopus and systematically adjusted. Parameters such as pulse duration, voltage, and pulse number were varied to find the most effective combination. The goal was to label single neurons without impacting neighboring cells. Following rigorous experimentation, the optimal SCE parameters for successful labelling of neurons were determined to be a single pulse of 15V for 30msec.

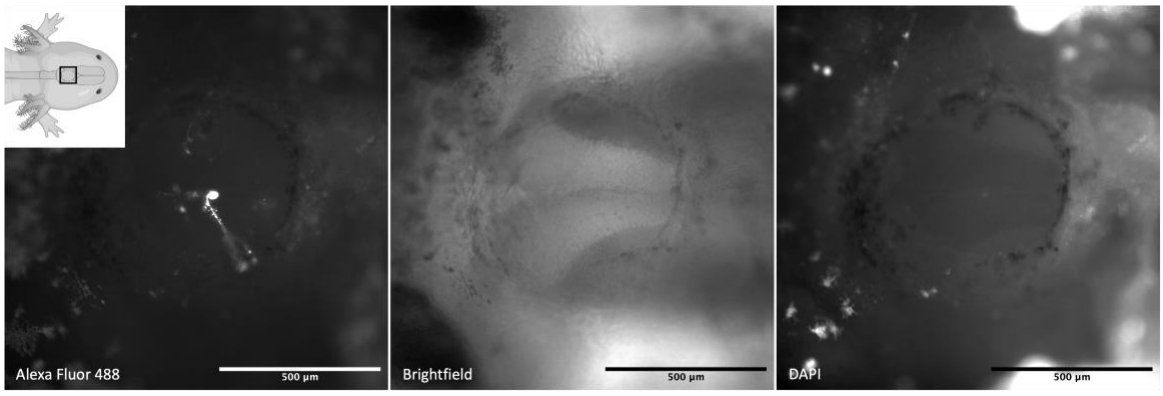

Figure 9: **Optimized single-cell electroporation labelling of a neuron in the axolotl optic tectum**. This image highlights the successful optimization of single-cell electroporation settings for labelling a neuron in the axolotl's optic tectum using dextran dye. Employing the optimized parameters (single pulse, 15V, 30msec), the left section demonstrates the neuron labelled with Alexa Fluor 488 dextran dye, providing clear and precise visualization four hours post SCE. The middle portion provides a bright-field channel image, offering context for the neuron's location within the brain tissue. On the right, the same brain region is displayed in the UV channel to validate the authenticity of the labelling signal, eliminating autofluorescence as a potential source. This optimized SCE approach is crucial for achieving precise neuronal labelling in the axolotl model.

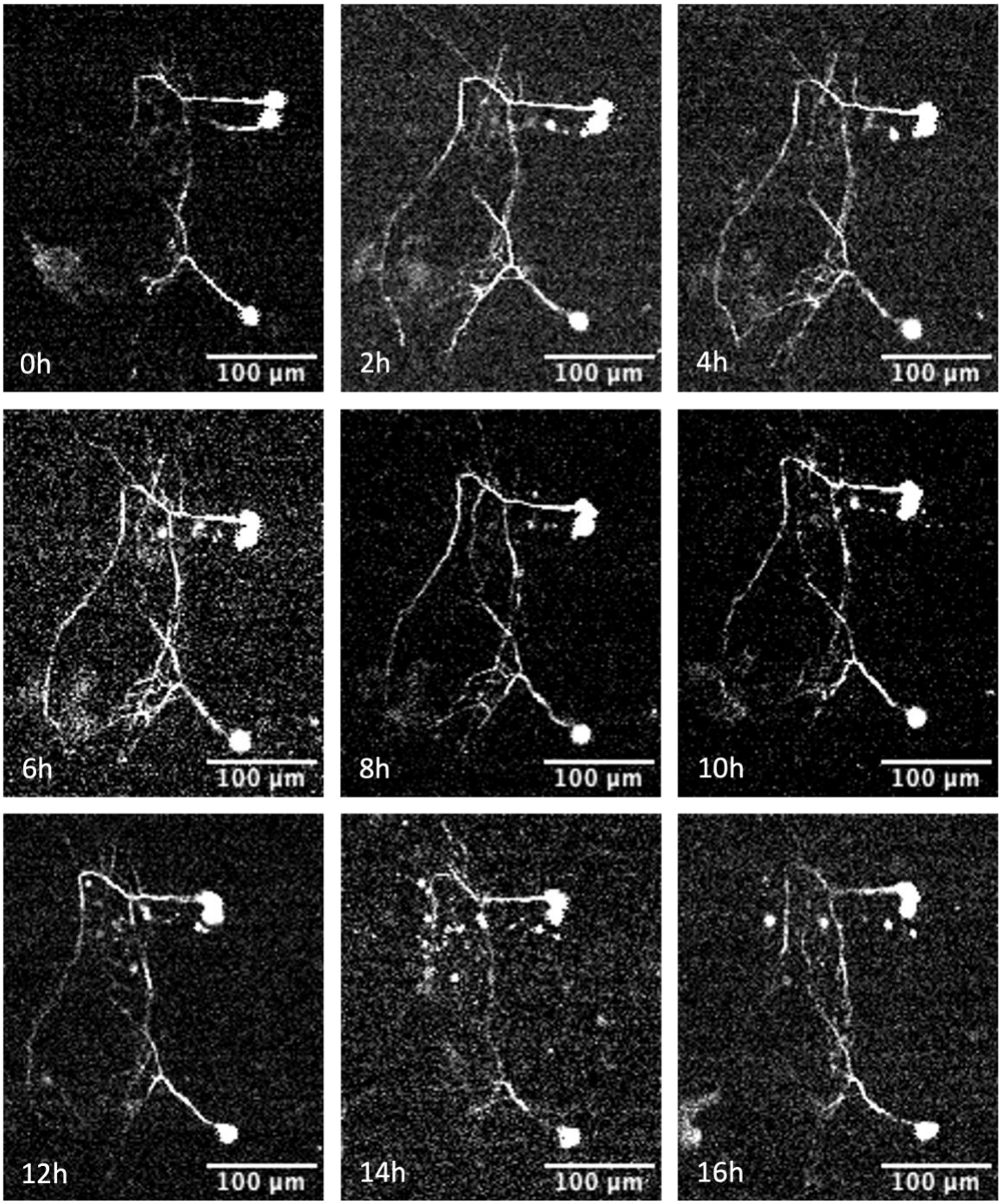

Figure 10: **Long-term live imaging of an electroporated single neuron**. In pursuit of effective neuronal labelling within axolotl neurons, initial Xenopus-based settings proved insufficient, with the signal fading rapidly within two hours post injection. Extensive experimentation led to optimized settings, featuring a single 15V pulse for a duration of 30msec. These settings, enabling effective labelling of optic tectum neurons, were validated via live imaging using a 2-photon microscope. Temporally, the signal increases for four hours post injection, followed by a decline from synapse to cell body.

After optimizing SCE for effective dye labelling in the axolotl brain, experiments attempted DNA-based SCE using parameters validated in *Xenopus laevis* (Liu and Haas, 2011b). These initial axolotl trials did not yet yield observable labelling within the brain. This underscores the need for continuing investigation and refinement to establish a dependable DNA delivery method through SCE tailored to the axolotl model.

Nevertheless, the transition to SCE marked an advancement in the ability to scrutinize individual neurons within the intricate neural networks of the axolotl brain. SCE's precision and control open new avenues to delve into neuronal development, connectivity, and function, as well as the dynamic interactions among individual neurons.

3.4 Precise labelling in the developing axolotl embryo

Following successful fine-tuning of the SCE settings to achieve precise neuronal labelling in the axolotl brain with dextran dye, investigations extended to target cells within the developing embryo. These experiments homed in stage 15 embryos, characterized by well-defined neuronal plate structures (Eagleson and Harris, 1990). This developmental stage provided an optimal context for electroporation procedures, enabling the introduction of fluorescent markers into individual cells. This controlled platform facilitates manipulations and systematic exploration of neural development, making it a pivotal phase for neurobiological studies.

Initial observations revealed that the labelling within epidermal cells remained detectable for a minimum of 7 days post injection (*Fig. 11*). However, ongoing studies in the laboratory are primarily dedicated to evaluating the persistence of the signal within neuronal tissue when targeting neuronal progenitor cells within the neural plate. This aspect presents a challenge because of a substantial yolk layer present within the cranial region of the axolotl embryo. Extending the observation timeframe is essential to furnish the necessary evidence confirming long-term effectiveness of dye-based SCE in the context of axolotl neuronal development.

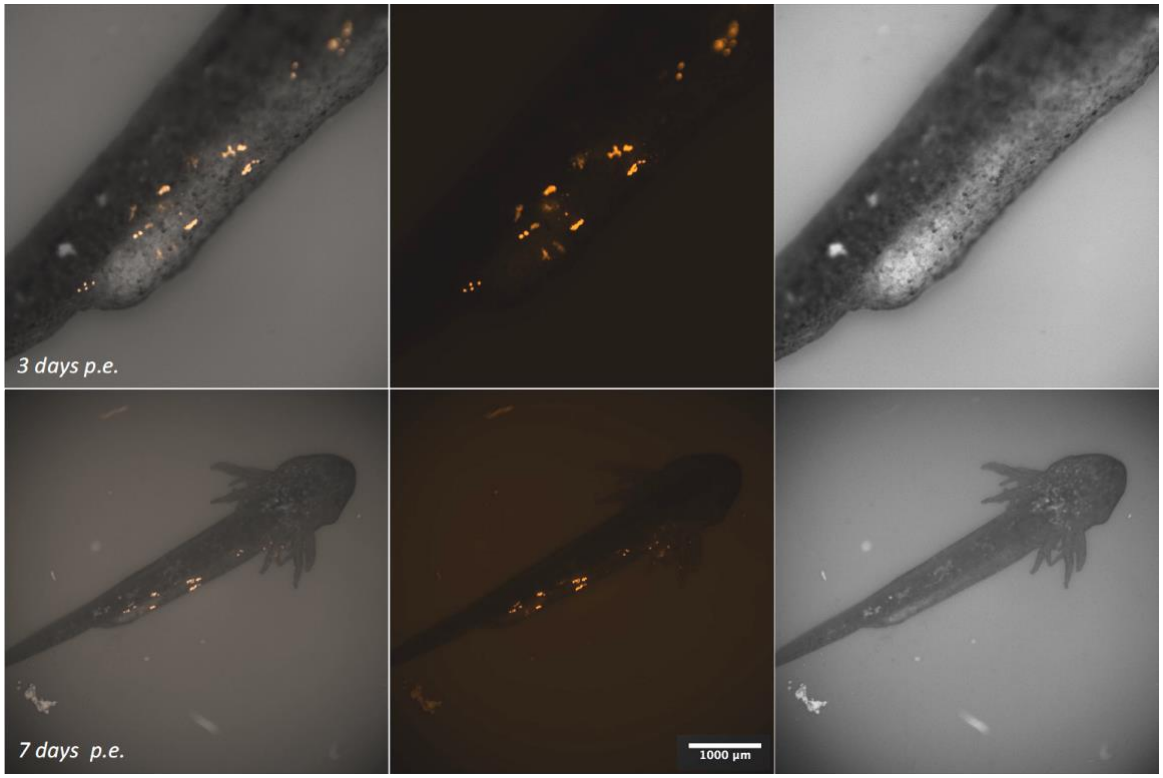

Figure 11: **Axolotl embryo development post electroporation**. The figure depicts an axolotl embryo at two time points: 3 days (*top row*) and 7 days (*bottom row*) post single-cell electroporation (SCE). Dorsal epidermal cells within the embryo are labelled with dextran dye (Alexa Fluor 555). This illustration demonstrates the enduring labelling capacity achieved by SCE with dextran dye. Imaging was conducted using a fluorescent microscope, with the left column displaying the observed embryo screen showing signal in dorsal epidermal cells. In the middle, the actual marker signal is shown, while the right column provides the autofluorescence control (UV channel).

4 Discussion

This study is leading towards deeper understanding of the intricate neurobiology of the axolotl (*Ambystoma mexicanum*). The aim was to employ single-cell electroporation and transposon technology to investigate the complex neuronal dynamics in the axolotl model. Key findings include: (1) Successful microinjection of genetic constructs for fluorescent labelling in developing axolotls thus validating the Tol2-mediated system. (2) Compatibility of genetic constructs for neuronal labelling within the axolotl brain using whole-brain electroporation (WBE), indicating their suitability for further experiments. (3) Single-cell electroporation (SCE) in the axolotl brain provided precise neuronal labelling, offering new opportunities to study individual neurons within complex neural networks. (4) While SCE using dextran dyes proved successful in the axolotl brain and embryo, the challenge persists with DNA-based markers, warranting further refinement. Collectively, these findings enhance the comprehension of axolotl neurobiology and offer promising directions for future research in this remarkable model organism.

4.1 Insights and challenges in genetic manipulation

Plasmids carrying various fluorescent membrane-tagged proteins were microinjected into axolotl eggs, along with Tol2 mRNA. This approach allowed to evaluate expression during development, assessing the suitability of these genetic constructs for long-term electroporation experiments. The expression of fluorescent proteins in cells led to diverse patterns across injected embryos, observed in gills, musculature, skin, and brain. Two weeks post injection, 89% of surviving axolotls displayed fluorescent signal in various tissues, indicating successful transfection.

It is worth noting that the percentage of positive embryos may be underestimated due to mosaic integration, a phenomenon where the introduced genetic material integrates variably into different cells, resulting in a weak signal in some tissues or within a subset of cells. Consequently, the fluorescent signal from these cells might not be easily detectable due to strong expression in surrounding tissues (as muscle seen in *Fig. 4* and *Fig. 6*). This

complexity posed challenges in precisely identifying which tissue acquired the transgene. To comprehensively assess the real expression pattern and the overall effectiveness of the Tol2-mediated approach, quantitative investigations would be necessary. However, for the purposes of this study, the conducted validation was sufficient to demonstrate the effectiveness of genetic expression throughout the embryo. Furthermore, mVenus-positive embryos continued to develop and displayed persistent expression patterns. This enduring expression provides compelling evidence for the successful transposon-mediated integration of genetic material into the host genome.

Upon further examination of single-plasmid injected embryos, positive signal was observed within the brain, suggesting successful labelling of neuronal tissue. To validate this integration into neuronal tissue, additional staining of neuronal cell bodies was performed (*Fig. 5*), confirming the utility of genetic markers for labelling neurons within the brain. To address challenges related to overexpression in surrounding tissues, further evaluation involved WBE to directly integrate genetic constructs into neuronal cells, using low concentrations of mGFP. Neuronal cell bodies and processes were labelled effectively, confirming the compatibility of transgenes for this purpose. Further reducing the concentration of injected plasmids would enable the co-injection of multiple transgenes, creating a 'brain-bow' like color diversity (Sakaguchi, Leiwe and Imai, 2018). This approach facilitates the simultaneous analysis of different neurons using distinct colors. This could contribute to the understanding of the projection map in the axolotl brain and offer insights into structural connectivity and neuronal dynamics.

Nevertheless, the provided findings collectively demonstrate evidence of successful expression of fluorescent membrane-tagged proteins within the axolotl brain, confirming the functionality and effectiveness of the genetic markers. This underscores the potential suitability of these constructs for single-cell electroporation experiments, facilitating targeted transfection within brain tissue and enabling precise cellular labelling.

4.2 SCE - Enhancing precision in axolotl neurobiology

Before applying the Tol2-mediated system for genetic labelling of individual neurons, the settings for SCE were adjusted based on previous work done in *Xenopus laevis* by Hewapathirane and Haas, 2008. Initially, high-voltage settings resulted in rapid cell death post-electroporation, suggesting the impact of electrical pulses on neurons. To optimize settings for immediate cell labelling without causing cell death, voltage, pulse number, and targeted sites within the brain were reduced. This allowed for stable and long-lasting dye labelling, enabling the evaluation of cell morphology and process orientation over time, as demonstrated by 2-photon live imaging in the optic tectum (*Fig. 10*).

Several factors might contributed to this, including phototoxicity resulting from prolonged exposure to fluorescent light sources (Tosheva *et al.*, 2020). To mitigate potential effects of phototoxicity, it is recommended to minimize exposure time during stereoscopic guidance and conduct screening as swiftly as possible (Icha *et al.*, 2017). On the contrary, long-term imaging experiments using 2-photon microscopy (*Fig. 10*) demonstrated sustained signal retention, which made phototoxicity unlikely to reason the cell death events. Another potential factor contributing to signal fading was tissue damage caused by the skull opening, which was not part of the original *Xenopus laevis* protocol but necessary in axolotls due to their thicker skin. Adjusting the micropipette was not feasible, and thinner or shorter needle tips proved damaging to brain tissue. To improve this, carefully carving a smaller incision site to access the sub-cranial region without exposing larger portions of the head, is potentially preventing the observed cell death due to tissue damage. Nevertheless, this technique offers studying morphological structural changes and neuronal analysis in the axolotl brain.

Further optimizations would allow for prolonged studies of morphological changes without altering the genetic landscape of neurons already done in *Xenopus laevis* (Haas *et al.*, 2002). Moreover, this could provide a powerful means to investigate brain connectivity, offering insights into neural circuitry, connectivity patterns, and functional roles within this model organism. Fluorescent markers enable to map neural connections, identify interconnected regions, and study projections within the axolotl brain. This

approach has potential to uncover how specific neural circuits contribute to various functions and behaviors, from sensory perception to motor control, and how they adapt and rewire in response to injury or environmental changes.

4.3 SCE - Precise labelling in the axolotl embryo

Building upon precise neuronal labelling within the axolotl brain using dextran dye, SCE was successfully used for labelling within the axolotl embryo. Initial trials in epidermal cells aimed to assess the adaptability of previously optimized settings for highly regenerative embryonic cells (Vieira, Wells and McCusker, 2020). These experiments focused on stage 15 embryos, tracking the longevity of fluorescent signal in successfully labelled cells. While the signal was detectable for a limited time during early development, the closure of the neural fold and the presence of a substantial yolk layer in the cranial region posed barriers to continued observation within the developing brain.

To further apply dye SCE in the neural plate, longer screening periods are necessary to determine if the injected signal persists in the brain as it does in epidermal cells during development. The enduring signal in embryonic cells further suggests that brain cell death might indeed be related to skull opening. The ability to label cells with dye over extended periods could be valuable for fluorescently tracking neuronal progenitors during development without genetic manipulation. It may also offer insights into fate map similarities with *Xenopus laevis* (Eagleson and Harris, 1990), opening new avenues for studying neuronal cell growth.

In summary, the extension of SCE to axolotl embryos holds promise for diverse applications in developmental and neurobiological research. The technique's adaptability to different tissues and the ongoing exploration of its long-term efficacy provides a strong foundation for future investigations into axolotl embryonic development and the broader applicability of SCE in this model organism.

4.4 Prospects in combining genetic constructs and SCE in axolotl

A more frontier ambition was to integrate the use of genetic constructs for fluorescent neuronal cell labelling with precise introduction into specific neuronal targets within the axolotl brain and embryo. However, several challenges were encountered during this investigation.

Initially, electric settings conventionally used for SCE of DNA in *Xenopus laevis* (Hossain, Podgorski and Haas, 2015) were applied to the axolotl. Under these settings, no gene expression was detected in the axolotl. Subsequently, systematic adjustments of electrical parameters might be necessary. Additional efforts could include mixing DNA with dextran dye, which facilitates the visualization of solution outflux and direct detection of uptake into the targeted cells (Bestman *et al.*, 2006; Steinmeyer and Yanik, 2012). This approach would aim to optimize SCE of the mixture to achieve genetic expression. Following this, the volume of dextran could be gradually diluted while further fine-tuning the electrical parameters. Despite these efforts, the optimal combination of settings may already be reached, but detection remained elusive due to the specific challenges associated with SCE in the axolotl brain, such as cell death as discussed before.

Moreover, multicolored labelling by targeting distinct cells with different transgenes presents an exciting avenue for studying neuronal projections and relationships between axolotl neurons. This 'brain-bow'-like approach could involve color-coding neighboring cells and tracking their projections (Steinmeyer and Yanik, 2012). Therefore, future investigations should prioritize the adaptability and optimization of DNA integration in the axolotl neural plate, considering the prolonged viability of injected cells compared to brain tissue, as demonstrated by SCE with dextran dye. Once it is established that DNA-based labelling within the brain can achieve long-lasting effects like those observed in the embryo, this approach may be effective to studying the axolotl brain, enhancing the understanding of neural projections and function (Haas *et al.*, 2002) in this remarkable model organism.

5 Outlook

The journey to enhance axolotl neurobiology, its regenerative capacities, and neuronal dynamics has been enriched through the innovative application of single-cell electroporation (SCE) in this study. The usage of dye markers and transposon-mediated integration of fluorescent proteins open exciting avenues for future research.

Comprehensive visualization of neuronal morphology: The refined SCE allows for direct visualization of cellular morphology within the axolotl brain. This provides the ability to study neuronal shape and structural orientation at an unprecedented level of detail. By examining variations between different brain regions, insights can be gained into how the axolotl manages complex neural processes and adapts post injury.

Monitoring neuronal growth and development: Extending SCE to the embryonic stage of axolotls presents an exciting opportunity to monitor the growth of neurons during development. This longitudinal approach enables the observation of how neurons mature throughout various stages of embryonic development. Such insights can relate to cellular mechanisms underlying regenerative capacities of axolotls.

Unraveling post-injury neural dynamics: SCE's application in specific brain areas, such as the hindbrain, offers a unique vantage point to observe and monitor ongoing reconstruction processed post-injury. By pairing SCE with concurrent behavioral experiments, dynamic changes occurring within these specific neural circuits could be elucidated. This integrated approach holds the potential to uncover novel insights into axolotl regeneration, shedding light on the intricacies of neural circuitry restoration.

Fine-tuning for precision: The ability to fine-tune stimulus parameters based on epifluorescence results is an asset in SCE. The labelling process may be optimized for other macromolecules by adjusting pulse parameters to achieve the desired level of fluorescence intensity and precision. This iterative approach ensures the precise targeting of individual cells to further introduce plasmid DNA carrying different genetic elements accurately.

The application of SCE in axolotl neurobiology marks a leap forward in the quest to understand neural structure, function, and regeneration. These advancements not only contribute to the knowledge of axolotl biology but also hold potential implications for neuroscience in a broader context. As research continues to evolve in this field, groundbreaking discoveries may inspire new avenues of exploration. Axolotls with their regenerative capacity remain a captivating model organism, and SCE is posed to unlock more of their secrets.

6 Conclusion

In the pursuit to offer a novel technique to unravel the neurobiology of the axolotl and harnessing its regenerative potential, this study embarked on a multifaceted journey. It aimed to seamlessly integrate macromolecules for fluorescent neuronal cell labelling with precise introduction into specific neuronal targets within the axolotl brain and embryo. The approach merged molecular manipulation with cutting-edge imaging techniques, yielding a powerful tool for examining morphological changes, growth patterns, and neuronal tissue rewiring post-injury. Key findings from this study have illuminated the path forward:

(1) **Validation of genetic constructs via microinjection**: Through microinjection, this study introduced genetic constructs for fluorescent labelling into developing embryos. This process, validating the Tol2-mediated system, provided a robust foundation for long-lasting experiments.

(2) **Genetic constructs for neuronal labelling in the axolotl brain**: Compatibility of these genetic constructs for neuronal labelling within the axolotl brain using whole-brain electroporation was demonstrated. This finding paves the way for further experiments exploring neuronal dynamics.

(3) **Precision and potential of single-cell electroporation (SCE)**: SCE introducing dextran dye in the axolotl brain and embryonic tissues emerged as a precise approach for neuronal labelling. These applications open new avenues for exploring the structural morphology of individual neurons within the intact brain and guide towards the visual evaluation of neuronal cell growth during development.

(4) **Challenges and prospects in DNA-based SCE**: While SCE using dextran dye proved successful in the axolotl model, the DNA-based approach posed various challenges. These include adjusting electrical parameters without visual guidance and addressing issues related to cell death.

Considering these findings, future investigations should focus on refining single-cell electroporation for long-term integration of Tol2-mediated DNA constructs in the axolotl embryo. The prolonged viability of injected cells within this tissue, as demonstrated by SCE with dextran dye, suggests that this avenue holds great promise. Moreover, as the longevity of labelled cells in the brain approaches that observed in the embryo, the DNA-based SCE could potentially be transferred to the axolotl brain, answering questions related to cellular reconstruction post-injury or individual cell responses to environmental cues.

This study underscores the remarkable potential of the axolotl as a model organism for neurobiological research and regenerative studies. The challenges encountered along the way serve as valuable guideposts for further refinement and innovation, ensuring that the quest to unravel the mysteries of axolotl neurobiology continues to advance, offering new insights into neural development, regeneration, and connectivity as proposed by Cajal.

7 References

Adamson, C.J., Morrison-Welch, N. and Rogers, C.D. (2022) 'The amazing and anomalous axolotls as scientific models', *Developmental Dynamics*, 251(6), pp. 922–933. Available at: https://doi.org/10.1002/dvdy.470.

Bae, C. and Butler, P.J. (2006) 'Automated single-cell electroporation', *BioTechniques*, 41(4), pp. 399–402. Available at: https://doi.org/10.2144/000112261.

Bestman, J.E. *et al.* (2006) 'In vivo single-cell electroporation for transfer of DNA and macromolecules', *Nature Protocols*, 1(3), pp. 1267–1272. Available at: https://doi.org/10.1038/nprot.2006.186.

Bölük, A., Yavuz, M. and Demircan, T. (2022) 'Axolotl: A resourceful vertebrate model for regeneration and beyond', *Developmental Dynamics*, 251(12), pp. 1914–1933. Available at: https://doi.org/10.1002/dvdy.520.

Combs, C.A. and Shroff, H. (2017) 'Fluorescence Microscopy: A Concise Guide to Current Imaging Methods', *Current Protocols in Neuroscience*, 79(1). Available at: https://doi.org/10.1002/cpns.29.

De Castro, F. (2019) 'Cajal and the Spanish Neurological School: Neuroscience Would Have Been a Different Story Without Them', *Frontiers in Cellular Neuroscience*, 13, p. 187. Available at: https://doi.org/10.3389/fncel.2019.00187.

Deng, R. *et al.* (2023) 'Cortical inhibitory but not excitatory synaptic transmission and circuit refinement are altered after the deletion of NMDA receptors during early development', *Scientific Reports*, 13(1), p. 656. Available at: https://doi.org/10.1038/s41598-023-27536-0.

Eagleson, G.W. and Harris, W.A. (1990) 'Mapping of the presumptive brain regions in the neural plate ofXenopus laevis', *Journal of Neurobiology*, 21(3), pp. 427–440. Available at: https://doi.org/10.1002/neu.480210305.

Echeverri, K., Fei, J. and Tanaka, E.M. (2022) 'The Axolotl's journey to the modern molecular era', in *Current Topics in Developmental Biology*. Elsevier, pp. 631–658. Available at: https://doi.org/10.1016/bs.ctdb.2021.12.010.

Escoffre, J.-M. *et al.* (2009) 'What is (Still not) Known of the Mechanism by Which Electroporation Mediates Gene Transfer and Expression in Cells and Tissues', *Molecular Biotechnology*, 41(3), pp. 286–295. Available at: https://doi.org/10.1007/s12033-008-9121-0.

Faulkner, R.L. *et al.* (2021) 'Application of Recombinant Rabies Virus to *Xenopus* Tadpole Brain', *eneuro*, 8(4), p. ENEURO.0477-20.2021. Available at: https://doi.org/10.1523/ENEURO.0477-20.2021.

Fei, J.-F. *et al.* (2014) 'CRISPR-mediated genomic deletion of Sox2 in the axolotl shows a requirement in spinal cord neural stem cell amplification during tail regeneration', *Stem Cell Reports*, 3(3), pp. 444–459. Available at: https://doi.org/10.1016/j.stemcr.2014.06.018.

Furuya, M. *et al.* (2003) 'Electroporation of cynomolgus monkey embryonic stem cells', *genesis*, 37(4), pp. 180–187. Available at: https://doi.org/10.1002/gene.10246.

Garcia-Lopez (2010) 'The histological slides and drawings of Cajal', *Frontiers in Neuroanatomy* [Preprint]. Available at: https://doi.org/10.3389/neuro.05.009.2010.

Ghosh, S.K. (2020) 'Camillo Golgi (1843-1926): scientist extraordinaire and pioneer figure of modern neurology', *Anatomy & Cell Biology*, 53(4), pp. 385–392. Available at: https://doi.org/10.5115/acb.20.196.

Gresens, J. (2004) 'An Introduction to the Mexican Axolotl (Ambystoma mexicanum)', *Lab Animal*, 33(9), pp. 41–47. Available at: https://doi.org/10.1038/laban1004-41.

Gross, M. (2018) 'Regeneration lessons from the axolotl', *Current Biology*, 28(5), pp. R187–R189. Available at: https://doi.org/10.1016/j.cub.2018.02.033.

Haas, K. *et al.* (2002) 'Targeted electroporation in Xenopus tadpoles in vivo – from single cells to the entire brain', *Differentiation*, 70(4–5), pp. 148–154. Available at: https://doi.org/10.1046/j.1432-0436.2002.700404.x.

Hanahan, D. (1983) 'Studies on transformation of Escherichia coli with plasmids', *Journal of Molecular Biology*, 166(4), pp. 557–580. Available at: https://doi.org/10.1016/S0022-2836(83)80284-8.

Hewapathirane, D.S. and Haas, K. (2008) 'Single Cell Electroporation in vivo within the Intact Developing Brain', *Journal of Visualized Experiments*, (17), p. 705. Available at: https://doi.org/10.3791/705.

Hickey, S.M. *et al.* (2021) 'Fluorescence Microscopy—An Outline of Hardware, Biological Handling, and Fluorophore Considerations', *Cells*, 11(1), p. 35. Available at: https://doi.org/10.3390/cells11010035.

Hossain, S., Podgorski, K. and Haas, K. (2015) 'Single-Cell Electroporation for In Vivo Imaging of Neuronal Morphology and Growth Dynamics', in B.R. Arenkiel (ed.) *Neural Tracing Methods*. New York, NY: Springer New York (Neuromethods), pp. 101–116. Available at: https://doi.org/10.1007/978-1-4939-1963-5_5.

Icha, J. *et al.* (2017) 'Phototoxicity in live fluorescence microscopy, and how to avoid it', *BioEssays*, 39(8), p. 1700003. Available at: https://doi.org/10.1002/bies.201700003.

Karra, D. and Dahm, R. (2010) 'Transfection Techniques for Neuronal Cells: Table 1.', *The Journal of Neuroscience*, 30(18), pp. 6171–6177. Available at: https://doi.org/10.1523/JNEUROSCI.0183-10.2010.

Kawakami, K. (2007) 'Tol2: a versatile gene transfer vector in vertebrates', *Genome Biology*, 8(Suppl 1), p. S7. Available at: https://doi.org/10.1186/gb-2007-8-s1-s7.

Keener, D.G., Cheung, A. and Futai, K. (2020) 'Single-Cell Electroporation across Different Organotypic Slice Culture of Mouse Hippocampal Excitatory and Class-Specific Inhibitory Neurons', *Journal of Visualized Experiments*, (164), p. 61662. Available at: https://doi.org/10.3791/61662.

Keller, R.E., Löfberg, J. and Spieth, J. (1982) 'Neural crest cell behavior in white and dark embryos of Ambystoma mexicanum: Epidermal inhibition of pigment cell migration in the white axolotl', *Developmental Biology*, 89(1), pp. 179–195. Available at: https://doi.org/10.1016/0012-1606(82)90306-2.

Kumar, P., Nagarajan, A. and Uchil, P.D. (2019) 'Electroporation', *Cold Spring Harbor Protocols*, 2019(7), p. pdb.top096271. Available at: https://doi.org/10.1101/pdb.top096271.

Kunieda, T. and Kubo, T. (2004) 'In vivo gene transfer into the adult honeybee brain by using electroporation', *Biochemical and Biophysical Research Communications*, 318(1), pp. 25–31. Available at: https://doi.org/10.1016/j.bbrc.2004.03.178.

Liu, X.F. and Haas, K. (2011a) 'Single-Cell Electroporation in *Xenopus*', *Cold Spring Harbor Protocols*, 2011(9), p. pdb.top065607. Available at: https://doi.org/10.1101/pdb.top065607.

Liu, X.F. and Haas, K. (2011b) 'Single-Cell Electroporation of *Xenopus* Tadpole Tectal Neurons', *Cold Spring Harbor Protocols*, 2011(9), p. pdb.prot065615. Available at: https://doi.org/10.1101/pdb.prot065615.

Llinás, R.R. (2003) 'The contribution of Santiago Ramon y Cajal to functional neuroscience', *Nature Reviews Neuroscience*, 4(1), pp. 77–80. Available at: https://doi.org/10.1038/nrn1011.

Luft, C. and Ketteler, R. (2015) 'Electroporation Knows No Boundaries: The Use of Electrostimulation for siRNA Delivery in Cells and Tissues', *SLAS Discovery*, 20(8), pp. 932–942. Available at: https://doi.org/10.1177/1087057115579638.

Lust, K. *et al.* (2022) 'Single-cell analyses of axolotl telencephalon organization, neurogenesis, and regeneration', *Science*, 377(6610), p. eabp9262. Available at: https://doi.org/10.1126/science.abp9262.

Maden, M., Manwell, L.A. and Ormerod, B.K. (2013) 'Proliferation zones in the axolotl brain and regeneration of the telencephalon', *Neural Development*, 8(1), p. 1. Available at: https://doi.org/10.1186/1749-8104-8-1.

Matsumoto, K. *et al.* (2019) 'Advanced CUBIC tissue clearing for whole-organ cell profiling', *Nature Protocols*, 14(12), pp. 3506–3537. Available at: https://doi.org/10.1038/s41596-019-0240-9.

Nowoshilow, S. *et al.* (2018) 'The axolotl genome and the evolution of key tissue formation regulators', *Nature*, 554(7690), pp. 50–55. Available at: https://doi.org/10.1038/nature25458.

Peron, M. *et al.* (2020) 'The stem-like STAT3-responsive cells of zebrafish intestine are WNT/β-catenin dependent', *Development*, p. dev.188987. Available at: https://doi.org/10.1242/dev.188987.

Peters, A. (2007) 'Golgi, Cajal, and the fine structure of the nervous system', *Brain Research Reviews*, 55(2), pp. 256–263. Available at: https://doi.org/10.1016/j.brainresrev.2006.12.002.

Potter, H. and Heller, R. (2018) 'Transfection by Electroporation', *Current Protocols in Molecular Biology*, 121(1). Available at: https://doi.org/10.1002/cpmb.48.

Sakaguchi, R., Leiwe, M.N. and Imai, T. (2018) 'Bright multicolor labeling of neuronal circuits with fluorescent proteins and chemical tags', *eLife*, 7, p. e40350. Available at: https://doi.org/10.7554/eLife.40350.

Sariyer, I.K. (2013) 'Transfection of Neuronal Cultures', in S. Amini and M.K. White (eds) *Neuronal Cell Culture*. Totowa, NJ: Humana Press (Methods in Molecular Biology), pp. 133–139. Available at: https://doi.org/10.1007/978-1-62703-640-5_11.

Schreckenberg, G.M. and Jacobson, A.G. (1975) 'Normal stages of development of the axolotl, Ambystoma mexicanum', *Developmental Biology*, 42(2), pp. 391–399. Available at: https://doi.org/10.1016/0012-1606(75)90343-7.

Schuez, M. and Sandoval-Guzmán, T. (2023) 'Axolotl Transgenesis via Injection of I-SceI Meganuclease or Tol2 Transposon System', in A.W. Seifert and J.D. Currie (eds) *Salamanders*. New York, NY: Springer US (Methods in Molecular Biology), pp. 321–333. Available at: https://doi.org/10.1007/978-1-0716-2659-7_21.

Steinmeyer, J.D. and Yanik, M.F. (2012) 'High-Throughput Single-Cell Manipulation in Brain Tissue', *PLoS ONE*. Edited by M. Giugliano, 7(4), p. e35603. Available at: https://doi.org/10.1371/journal.pone.0035603.

Summers, D.K. (1996) *The biology of plasmids*. Osney, Oxford OX ; Cambridge, Mass: Blackwell Science.

Tazaki, A., Tanaka, E.M. and Fei, J.-F. (2017) 'Salamander spinal cord regeneration: The ultimate positive control in vertebrate spinal cord regeneration', *Developmental Biology*, 432(1), pp. 63–71. Available at: https://doi.org/10.1016/j.ydbio.2017.09.034.

Tolmasky, M. and Alonso, J.C. (eds) (2015) *Plasmids: biology and impact in biotechnology and discovery*. Washington, DC: ASM Press.

Tosheva, K.L. *et al.* (2020) 'Between life and death: strategies to reduce phototoxicity in super-resolution microscopy', *Journal of Physics D: Applied Physics*, 53(16), p. 163001. Available at: https://doi.org/10.1088/1361-6463/ab6b95.

Venkataramani, P.V. (2010) ‘Santiago Ramón y Cajal: Father of neurosciences’, *Resonance*, 15(11), pp. 968–976. Available at: https://doi.org/10.1007/s12045-010-0113-6.

Vieira, W.A., Wells, K.M. and McCusker, C.D. (2020) ‘Advancements to the Axolotl Model for Regeneration and Aging’, *Gerontology*, 66(3), pp. 212–222. Available at: https://doi.org/10.1159/000504294.

Voss, S.R., Epperlein, H.H. and Tanaka, E.M. (2009) ‘*Ambystoma mexicanum* , the Axolotl: A Versatile Amphibian Model for Regeneration, Development, and Evolution Studies’, *Cold Spring Harbor Protocols*, 2009(8), p. pdb.emo128. Available at: https://doi.org/10.1101/pdb.emo128.

Wang, M. *et al.* (2010) ‘Single-cell electroporation’, *Analytical and Bioanalytical Chemistry*, 397(8), pp. 3235–3248. Available at: https://doi.org/10.1007/s00216-010-3744-2.

Weaver, J.C. (1995) ‘Electroporation Theory: Concepts and Mechanisms’, in Nickoloff, J. A., *Animal Cell Electroporation and Electrofusion Protocols*. New Jersey: Humana Press, pp. 3–28. Available at: https://doi.org/10.1385/0-89603-304-X:3.

Yuste, R. (2015) ‘From the neuron doctrine to neural networks’, *Nature Reviews Neuroscience*, 16(8), pp. 487–497. Available at: https://doi.org/10.1038/nrn3962.

Zhang, Z., Zheng, T. and Zhu, R. (2020) ‘Single-cell individualized electroporation with real-time impedance monitoring using a microelectrode array chip’, *Microsystems & Nanoengineering*, 6(1), p. 81. Available at: https://doi.org/10.1038/s41378-020-00196-0.

8 Appendix

8.1 Deutsche Zusammenfassung

In dieser Masterarbeit und der zugrundeliegenden Studie wurde die zelluläre Markierung im Gehirn und embryonalen Gewebe des Axolotls durch single-cell electroporation (SCE) optimiert. Anfängliche Untersuchungen konzentrierten sich auf die Mikroinjektion einzelner Plasmide in Zygoten, um die Transposon-vermittelte Integration fluoreszent membran-bindender Proteine in der embryonalen Entwicklung zu evaluieren. Anschließend wurde mittels whole-brain electroporation (WBE) die Kompatibilität dieser genetischen Konstrukte für die Integration in neuronale Zellen untersucht. Weitere Untersuchungen zeigten, dass SCE mit Dextran-Farbstoff eine effektive Methode bietet, um die strukturelle Morphologie von Axolotl-Neuronen mit bemerkenswerter Präzision zu erforschen.

Diese Ergebnisse bestätigten die Wirksamkeit von SCE bei der Markierung einzelner Neuronen im Axolotl-Gehirn und -Embryo. Dies öffnet neue Möglichkeiten, strukturelle Dynamiken im Gehirn und das neuronale Wachstum während der embryonalen Entwicklung zu untersuchen. Zukünftige Untersuchungen, die die Langlebigkeit der genetischen Konstrukte mit der Effizienz von SCE kombinieren, versprechen große Fortschritte in der Axolotl-Neurobiologie, insbesondere im Zusammenhang mit der Regeneration des Nervengewebes.

8.2 Axolotl transgenesis - How to inject embryos

(Tobias Richter, 23.08.2006 / Update by Yuka Taniguchi-Sugiura, 19.07.2018)

Equipment and Materials:

- White boxes (A.Hartenstein, S50)
- Petri dishes with cams (60mm, 90mm, 150mm - available in the IMP store)
- Metal sieve (Carl Roth, 8098.1)
- Tweezers (3 of sharp, Fine science tools, #5 forceps)
- Stereo scopes (Olympus, SZX10)
- Micro manipulator (Narishige, MN-153) + Magnetic Stand (GJ-1) + Iron plate
- Glass needles (capillaries) (Harvard Apparatus, No. GC100F-15, with Filament)
- Pipette tips
- Microloader (Eppendorf, 5242956003)
- Glass bottles
- Mold made by Silicone (Sylgard 184)
- Stage Micrometer (Fine Science Tools, 29025-01)
- Filter Cup (0.2µm - available in the IMP store)
- 24-well plate (available in the IMP store)
- 10xMMR (IMBA/IMP Media kitchen)
- Ficoll400 (GE17-0300-05, Sigma-Aldrich)
- Penicillin-Streptomycin (PU781-100ML, Sigma - available in the IMP store)
- Sodium hypochlorite (71696-2.5L, -10% at RT, Honeywell- store at cold room)
- Plasmid DNA
- Tol II RNA for standard transgenesis B

To be made in advance:

- Glass needles
- 1xMMR + pen-strep
- 0.1xMMR + pen-strep
- 20%Ficoll/1x MMR + pen-strep
- 5%Ficoll/0.1x MMR + pen-strep
- Tol II RNA for standard transgenesis (store at -80°C freezer)

Recipes:

10xMarc's Modified Ringers (MMR), pH7.8: available at IMBA/IMP media kitchen.

	Final Concentration
NaCl	1M
KCl	20mM
$MgCl_2$	10mM
$CaCl_2$	20mM
EDTA	0.1mM
HEPES	50mM

1xMMR/pen-strep

	for 1l
10x MMR	100ml
MilliQ water	up to 1l

- Autoclave
- Add 10ml of Penicillin-Streptomycin
- Store at 4°C

1xMMR/20%Ficoll/pen-strep

	for 1l
10x MMR	100ml
MilliQ water	up to 500ml
Ficoll 400	200g

- Add stir bar and shake by hand. Stir on magnetic stirrer.
- Add MilliQ water (up to 1l)
- Add 10ml of Penicillin-Streptomycin
- Filter sterile
- Store at 4°C

0.1xMMR/5%Ficoll/pen-strep

	for 1l
10x MMR	10ml
MilliQ water	up to 500ml
Ficoll 400	50g

- Add stir bar and shake by hand. Stir on magnetic stirrer.
- Add MilliQ water (up to 1l)
- Add 10ml of Penicillin-Streptomycin
- Filter sterile
- Store at 4°C

0,1xMMR/pen-strep

	for 1l
10x MMR	10 ml
MilliQ water	up to 1l

- Autoclave
- Add 10ml of Penicillin-Streptomycin
- Store at 4°C

Standard injection mix

*for **0,5 ng** per embryo and **5 nl** injection volume:*

DNA	100ng
Tol II RNA	500ng
DNase/RNase-free Water	up to 10µl

Procedure:

On the day of injection:

1. Pick up eggs from the colony.
2. Store them in the 10°C fridge.
3. Prepare Sodium hypochlorite (2x 500 ml), 1x MMR/pen-strep (100ml) in beaker.

Sodium hypochlorite (10%)	0.3ml
Tap water	up to 1l

4. Pour off the eggs to metal sieve and rinse with clean lab-H_2O thoroughly.
5. Place the eggs in Sodium hypochlorite, allow them to stand 5 min.
6. Pour off the eggs to metal sieve and rinse with clean lab-H_2O thoroughly.
7. Repeat steps 5 and 6.
8. Place the eggs in 1xMMR/pen-strep.
9. Dejelly them very carefully with two sharp tweezers under stereoscope.
10. Collect dejellied eggs in another Petri dish in 1xMMR/pen-strep and keep them in the 10°C fridge until you inject them.

11. Before you go to the injection scope, prepare all needed things:

    a. injection mix
    b. needles*
    c. silicone mold
    d. small petri-dishes
    e. sterile pipettes (2ml)
    f. one tweezers for break needle (not the ones used for dejelling)
    g. stage micrometer to determine the volume of the injection-droplet

Pulling of the needles: Micropipette Puller (Sutter Instrument P-97)*

Program	No. 56
P	500
Heat	Ramp Value + 30
Pull	100
Velocity	120
Time	150

12. Wash silicone mold with deionized water, spray 70% EtOH, and rinse again with deionized water.

13. Fill silicone mold with 20%Ficoll/1xMMR/pen-strep (about 10ml).

14. Back-fill the needle with the injection solution by using Eppendorf microloader and mount the needle in the micromanipulator.

15. Break very tip of the needle with tweezers and remove bubbles from needle tip.

16. Check the volume of the droplet (see Table 1). Break more if necessary. But don't break too much, otherwise the hole will be too big and you will destroy the embryo. If the volume is still too little, break the needle tip a little bit more.

    - Calculating microinjection volumes:

Diameter of drops (µm)	Volume of drops (nl)
125	1.03
140	1.44
150	1.77
160	2.15
170	2.58

- PicoPump settings for egg injection:

Strength of air pressure	2 Bar
Eject	26
Range	100msec
Period	10
Duration	Timed

17. Transfer healthy-looking eggs into the injection mold filled with Ficoll/1xMMR pen strep.

18. Inject solution into eggs.

19. Transfer injected eggs in another Petri dish filled with 20%Ficoll/1xMMR/pen-strep. Go on, until you have injected the desired number of embryos.

20. Two hours after injection, transfer the embryos into a big Petri dish filled with 5%Ficoll/0.1xMMR/pen-strep. Store those dishes at RT or in the 16°C incubator.

Next day of injection:

21. Transfer healthy-looking eggs in 24-well plates filled with 0.1xMMR/pen-strep. Store those plates at RT or in the 16°C incubator.

Few days to 2 weeks after injection:

22. Check survivability and strength of transgenic efficiency under the fluorescence microscope.

23. Transfer healthy/positive embryos into tap water.

8.3 How to label single neurons in the axolotl brain with Dextran Dye

Reagents

Anesthesia - 0.03% Benzocaine (Khattak et al., 2013 Nature Protocol)

1xPBS (IMP Media Lab, https://medialab.vbc.ac.at/Products/2)

Delivery molecules solution (Dextran Dye Alexa 488/555, Thermo Fischer, D22910/D34679, Aliquot = 10 µg/µl Milli Q Water 5µl/tube)

Equipment

Electrical stimulator (A-M Systems Isolated Pulse Stimulator Model 2100)

Fluorescence Stereo Zoom Microscope (Zeiss Axio Zoom.V16)

Glass capillaries for pipettes (Boroscilicate - Standard wall w/filament G150F-2,

OD = 1.50mm, ID = 0.86mm, Length = 7.5cm, www.warneronline.com 203-776-0664)

Micro Centrifuge (LLG-uniCFUGE 2)

Microelectrode holder (www.wpiinc.com/var-3822-microelectrode-holder-mph6r.html)

Micromanipulator, three-axis coarse (NARISHIGE MN-153)

Microscope for SCE (Olympus LED Transmitted Light Illumination Base SZX2-ILLT,

Olympus Wide Zoom Stereo Microscope SZX16)

Oscilloscope (Tektronix TBS 1000C Series Digital Oscilloscope)

Petri dish (size fitting used animals)

Pipette holder with silver wire

Pipette puller (Sutter instrument P-97)

Scalpel with pointed end

Silver wire (www.wpiinc.com/var-2288-bare-silver-wire.html)

Transfer pipette

Tube loader pipette tips

Tweezers (round tips, sharp tips)

Single-cell electroporation setup

1. Pull pipettes on a horizontal micropipette puller.
(Heat = Ramp, Pull = 0, Velocity = 45, Delay = 1, Loops = 4; Program 51)
2. Briefly centrifuge the solution(s) of desired molecules at high speed to reduce the amount of particulate debris drawn into the micropipette.
3. Fill a petri dish with 1x PBS and place the silver wire electrode in contact with the PBS. Connect the wire electrode with the stimulator using the red cable hook.
4. Fill a micropipette with solution of desired molecules either by backfilling (i.e., dipping the non-tip end into the filling solution and allowing it to fill by capillary action) or by direct injection using a thin tube loader so the wire is in contact with the solution.
Avoid bubbles in the tip. If bubbles occur, dislodge by vigorously flicking the pipette.
5. Insert the micropipette into a holder mounted on a three-axis coarse micromanipulator. Ensure that the silver wire electrode inserted into the micropipette is in contact with the filling solution. Connect the wire electrode with the stimulator using the black cable.

Procedure

6. Anesthetized axolotls in diluted Benzocaine.
7. Transfer a single anesthetized axolotl into the PBS filled petri dish using round tip tweezers.
8. Carefully pocking the axolotl's head with a scalpel behind the optic tectum and open the skull using sharp tweezers to access the brain area of interest.
9. Under the microscope, carefully position the pipette tip above the target region in the axolotl brain. Slowly lower the micropipette until it touches the surface layer of the brain.
10. Pause for a moment before applying stimulation to allow the tissue to resettle.
11. Apply electric stimulation to the axolotl (30 msec pulse with 15V).
12. Withdraw the pipette from the brain and move it to another appropriate site.
13. Repeat steps 9 to 12.
14. Return the axolotl into tap water to allow it to recover.
15. Repeat steps 8 to 14 using another anesthetized axolotl.

Screening

16. Anesthetize axolotl in diluted Benzocaine.
17. Place the axolotl in a petri dish and on the stage of a fluorescence stereomicroscope or the Axiozoom and rapidly screen for successful labelling using the desired excitation light.

8.4 CUBIC protocol for antibody staining

Updated 31.03.2023

Solutions:

Bleaching solution

Ingredient	%w	eg for 200ml
H_2O_2	3	6ml
KOH	0.5	1g
PBS-Triton (0.2%)		up to 200 ml

CUBIC-L

Ingredient	%w	eg for 500g
Triton X-100	10	50g
N-butyldiethanolamine	10	50g
dH_2O		up to 500 g

- Can be stored at RT for up to 6 months.
- As can the half-diluted CUBIC-L.

CUBIC-R1a

Ingredient	%w/v	eg for 500g
Urea	10	50g
N,N,N',N'-tetrakis	5	25g
Triton X-100	10	50g
5M NaCl	1:200	2.5ml
dH_2O		up to 500ml

- An unpublished reagent, available at http://www.cubic.riken.jp

RI matching solution CUBIC-R+(N)

Ingredient	%w	eg for 100g
Antipyrine	45	45g
Nicotinamide	30	30g
dH_2O		25g

- After complete dissolution, add 500µl of *N*-butyldiethanolamine to the 100ml mixture and adjust the pH to 9.6 - 9.8. The RI should be 1.522. Worth checking occasionally.
- CUBIC-R+(N) can be stored at RT for up to 6 months.

Procedure:

1. Fix the embryos/brains overnight in 4% PFA (paraformaldehyde) at 4°C.
2. 6 washes, 30 min each with PBST (0.2% Triton) at 4°C.
3. Dehydration in methanol at 4°C (optional for long term storage):

   25% in 1xPBS, 50% in 1xPBS, 75% in 1xPBS and 2x100% -> store at -20°C

   -> Rehydration reverse in same solutions
4. Depigmentation (helps also for reducing blood cell autofluorescence) with bleaching solution for roughly 1 hour on a shaker at RT (check after 30 minutes).
5. Wash 3x in PBST for 10 minutes at RT
6. Delipidation:

   - 50% CUBIC-L/R1a solution (mixed 1:1 then diluted to 50% in dH_2O) 30min at RT

   - 100% CUBIC-L/R1a solution 1 hour, on a shaker at 37°C
7. 4x washes, 20min each with PBST at RT
8. Blocking: 4% Goat Serum, 1% DMSO in PBST -> 1 hour at RT on shaker
9. Antibody in 4% Goat Serum, 1% DMSO in PBST, 6 over nights on shaker at 4°C
10. Wash 6x 30 min with PBST on shaker at RT
11. RI matching in CUBIC-R(+N) solution -> on shaker at RT until transparent
12. Image